# Hydrochemical and Environmental Isotope Based Investigation of the Masama Ntane Sandstone Aquifer, Botswana

by

Thelma Mofokeng

(1505796)

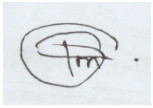

……

A Thesis Submitted to the Faculty of Science

SCHOOL OF GEOSCIENCES

In Partial fulfillment of the Requirements for the Degree of

MASTERS OF SCIENCE IN HYDROGEOLOGY

Supervisor: Prof. Tamiru Abiye

June 2017

STATEMENT BY AUTHOR

This thesis has been submitted in partial fulfillments of requirements for an advanced degree at The University of the Witwatersrand.

. SIGNED:… 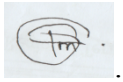 ……..

APPROVAL BY THESIS DIRECTOR

This thesis has been approved on the date below:

…… 01/06/2017

Tamiru Abiye Date

Professor of Hydrogeology

## ACKNOWLEGDEMENTS

I am grateful to my advisor and lecturer Professor Tamiru Abiye for his patience and laboratory assistance in this long tough journey and for all the wisdom he bestowed upon during the course of the project. Special thanks to Ithemba laboratory, Gauteng, especially Mr Mike Butler for the radioisotope analysis and Water Utilities Corporation Laboratory for water analysis results and permission to sample their boreholes.

Heartfelt thanks to Water surveys Botswana management for the project sponsorship, my technical supervisor Mr R. Hunt and Masama project team members: Mr A. Preston, Ms M. Motsumi and Mr F. Tego for their technical support.

Abstract

The Masama Sandstone Aquifer is located in a semi-arid region of south-eastern Botswana where there are no perennial rivers. Groundwater is the main source of water supply for the communities. Historically many water drilling programs have been carried out in this area and the hydrogeological system has been conceptualized. An integrated approach coupling environmental isotopes, radioisotopes and multivariate statistical analysis of the hydrochemical variables was employed to study the origin, age, recharge conditions, rock-water interaction and the hydrological link between the aquifer and geological structures. The major ions in this area are $Na^{+}$, $Ca^{2+}$, $Mg^{2+}$ and $HCO^{-}_{3}$. Groundwater in the Masama area fall in the transition from a Na-$HCO^{-}_{3}$ –type through Ca-Na-$HCO^{-}_{3}$ to Ca-Mg-$HCO^{-}_{3}$ -type waters from the western to the eastern part of the area. The water types are as a result of cation exchange, carbonate dissolution and rock-weathering processes. The $\delta^{18}O$ and $\delta^{2}H$ values vary spatially depending on the source of moisture, rainfall season, geology, topography and groundwater circulation depth. Deep circulating groundwaters are isotopically depleted whilst shallow circulating groundwaters are isotopically enriched with respect to winter rain. Low tritium values < 0.8TU and $^{14}C$ values < 80pmc testifies for recharge. Recent rainfall amount in the area is not sufficient enough to make a profound replenishment in the aquifer. Tritium, $^{14}C$ and Chloride Mass Balance helped in identifying recharge location and hydrologic connections between structures and the sandstone aquifer elucidating that recharge zones are in the NE and NW of the study area. High recharge rates occur in the north-eastern part and the Makhujwane fault act as a conduit for groundwater recharge. This study provides a better understanding of the aquifer and the information contained herein can be incorporated into future works for sustainable use of the groundwater resource.

## Table of Contents

LIST OF APPENDICES



LIST OF FIGURES

LIST OF TABLES



LIST OF PLATES



LIST OF ABBREVIATIONS

**$BaCO_3$** Barium Carbonate

**$^{14}C$** radiocarbon

**$Ca^{2+}$** Calcium

**$Ca^{+2}$-$HCO^{-}_{3}$** Calcium Bicarbonate

**Ca-Mg-HCO3** Calcium magnesium bicarbonate

**CCC** Consolidated Construction Company

**$Cl^{-}$** Chloride

**CMB** Chloride Mass Balance

**$CO_2$** Carbon dioxide

**$CO_3^{-2}$** Carbonate

**$^{2}H$** Deuterium

**$^{3}H$** Tritium

**$HCO_3^{-}$** Bicarbonate

**$H_2CO_3$** Carbonic acid

**DGS** Department Geological Surveys

**DIC** Inorganic carbon

**DOC** Dissolved organic carbon

**EC** Electrical conductivity

**ESE** East-South-East

**$F^{-}$** Fluoride

**GPS** Geographical Point System

**HCA** Hierarchical cluster analysis

**$H_2S$** Hydrogen sulphide

**ICP-OES** Induced Coupled Plasma Optical Emission Spectrometer

**k** Conductivity

**$K^{+}$** Potassium

**L** Litre

**LBMWL** Letlhakeng-Botlhapatlou Meteoric Water Line

**$Mg^{2+}$** Magnesium

**mg/l** milligram per litre

**MSA** Masama Sandstone Aquifer

**$Na^{+}$** Sodium

**$NO_3^{-}$** Nitrate

**nT** nanoTesla

**$^{18}O$** Oxygen-18

**PCA** Principal component analysis

**pmc** percent modern carbon

**PTFE** Polytetrafluoroethylene

**SDAT** Statistical Data Analysis Techniques

**S** storativity

**$SO_4^{-2}$** sulphate

**T** Transmissivity

**$T_D$** Total annual chloride deposition

**TDS** Total Dissolved Solids

**TU** Tritium Units

**WNW** West North West

**WSB** Water Surveys Botswana

**‰** permil

# 1 INTRODUCTION

Recent climatic variations that have been occurring around the world have led to most countries shifting their attention to groundwater as the major supply of water especially in arid and semi-arid areas (De Vries, 2000; Stephenson et al., 2004). Botswana being one of the countries in southern Africa that falls within the semi – arid climatic zone, receives low precipitation making surface water a negligible resource (DWA, 2006).With the major city being Gaborone, most people, industries and many villages are located around this area, which puts pressure on the water resource (WSB, 2015b).

The Masama area is located 100 km northeast of the city of Gaborone. The geology is primarily represented by the Karoo Supergroup rocks with the main water bearing unit belonging to the Ntane sandstone, which overlies the mudstone and is overlain by fractured amygdaloidal basalts. This sandstone aquifer has been studied by consultants and proved to have more groundwater resources that could be useful to sustain the population growth of Gaborone and surrounding villages. Around 1997 a wellfield was developed to supply water to the villages around the area and recently the wellfield is being extended to supply water to the greater Gaborone area to compliment for the water that has been supplied by Gaborone Dam, which is now dry.

An intrinsic approach that has gained increased attention in recent groundwater studies around the world involves the use of isotope technique to augment convectional hydrogeologic methods. This approach provides supplementary information, which is independent of hydraulic parameters, as isotope tracers look directly at the groundwater itself rather than at the rock through which the water flows.

Numerous authors (Vogel et al., 1982; Edmunds et al., 1988; Vandenschrick, 2002; Boronina et al., 2005; Yeh et al., 2009; Bakari et al., 2012, Jassas and Merkel, 2015) have used isotopes to conduct groundwater studies. Some of these studies focused on the determination of groundwater age, recharge mechanism, sources of recharge, groundwater connection between aquifers and processes affecting groundwater quality and the technique were useful and successful, thereby providing other means for investigating ways of assessing groundwater resources in large basins.

In Botswana, the use of isotopes is not routinely used as an analytical tool. Authors like Jennings (1970); Verhagen etal. (1975); Mazor and Sellschop (1977); Dincer et al. (1979); Verhagen (1990); Selaolo (1998) and De Vries (2000) have used isotopes in groundwater studies in the Kalahari region. Conventional hydrogeological techniques such as borehole drilling, water analysis, pumping tests and numerical modeling, have also been extensively used to understand the hydrogeological processes, water quality and groundwater flow regimes in this area, with every successive exploration program providing new findings that helped in reviewing of the data.

To understand and characterize the Masama Sandstone Aquifer (MSA), which is the main objective of this work, geochemical**,** hydrogeological and isotope data assessment was used in an integrated manner. This research entails an integrated approach of the aquifer in question.

### 1.1 Purpose and Scope

The wellfield, termed the Masama-Makhujwane Wellfield, comprised of some 37 production boreholes with the last batch drilled in 2014. The main water bearing unit in the wellfield area is the Ntane Sandstone, which is overlain by the thick amygdaloidal basalts and underlain by mudstones (WSB, 2015a). Most of the drilled boreholes were able to tap into this aquifer and a

transient model was simulated, which predicts water supply from this aquifer for the next 30 years (WSB, 2015b). In April 2016, drilling of an additional 25 production and 8 exploration boreholes was conducted forming a new wellfield to the west of Masama-Makhujwane Wellfield.

The combined wellfield will provide about 60 000$m^3$/day to the greater Gaborone (WSB, 2015a). Availability of more boreholes in comparison to the past provides an opportunity for application of other scientific techniques, which could have been inhibited by this limitation and a platform for understanding the spatial distribution of water quality and groundwater dynamics within the area as the good borehole coverage mimic a representation of the aquifer system. Data collected from drilling, pumping test and the model formed the basis of the current work.

For better management of the water resource, all possible scientific techniques should be examined to minimise any possibility for potential over-exploitation of the water resource. This can be achieved through the use of other techniques that have not been previously used.

### 1.1.1 Aims and Objective

The main aim of the study is to get a better understanding of the Masama Sandstone Aquifer (MSA) through the integrated use of environmental isotopes and hydrochemical data analysis of groundwater samples to acquire information that cannot be provided by traditional hydrological techniques with a view to provide additional information for future projects. To achieve this, the following objectives have been addressed:

- Determination of the processes governing the chemistry of the groundwater and the role played by the geologic structures in the study area.

- Qualitative and quantitative determination of the age of the groundwater while concurrently deducing potential recharge zones and sources.

## 1.2 Description of Study Area

### 1.2.1 Location of study area

The proposed area, Masama, is located 100 km to the north-east of the city of Gaborone and is on the eastern side of the Gaborone – Francistown main road (**Error! Reference source not found.**). The Masama-Makhujwane wellfield has an aerial coverage of approximately 3000 $km^2$. Around the area, there are small villages of Artesia to the southwest and Dibete to the North of the study area.

### 1.2.2 Physiography

The area is characterised as a plain that gently dips towards the Notwane valley to the southeast. The geomorphology is controlled by geological structures, characterised by occasional WNW-ESE ridges of aeolian Kalahari sand and linear topographic highs, which coincide with major fault zones (Khurutse, Boleleme and Masama Fault system) while the central part of Khurutse area has graben structures accounting for little topographic relief (WSB, 2015a).

The drainage system in the area is represented by an ephemeral Notwane river, which drains north-easterly into the Limpopo River (**Error! Reference source not found.**). Minimum elevation of about 900 masl is recorded along the Notwane river course with maximum elevation within the Khurutse area of 1040 masl north of Dibete village.

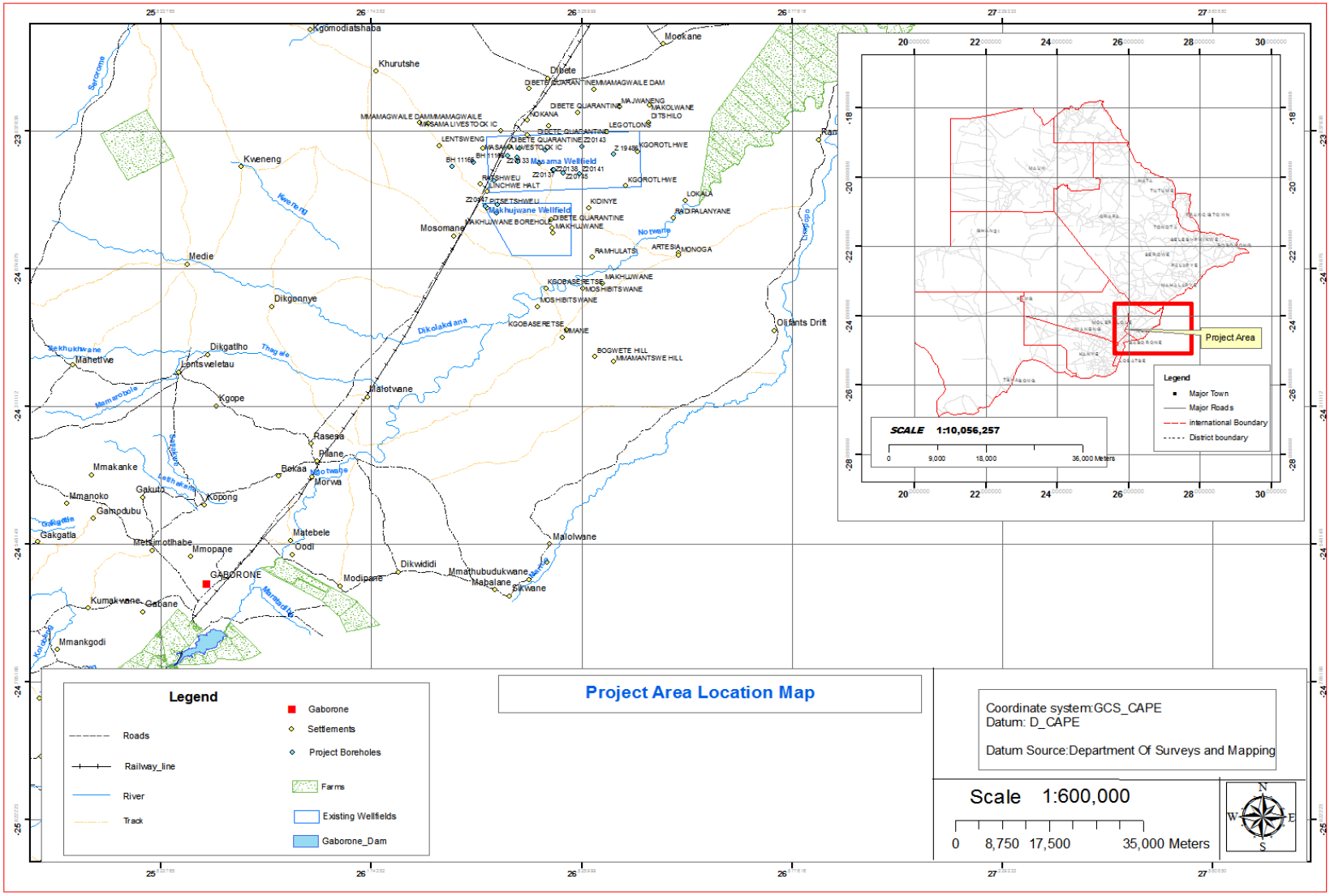


Figure 1.1 Project location Map

### 1.2.3 Climate, soils and vegetation

The study area falls to the south of the Tropic of Capricorn and is influenced by both the inter-tropical air masses and the southern polar oceanic air masses. The climate is semi-arid, with cold, dry winters and hot and wet summers. The rainfall pattern is similar to most areas in Botswana with most rain falling between November and February (DWA, 2006).

The area is characterized by the average and maximum rainfall, 393 mm/year and 656 mm/year, respectively as recorded at Dibete (Figure 1.2). The highest maximum monthly rainfall totals collected at the Consolidated Construction Company (CCC) are around 250 mm/month for the four wettest months.

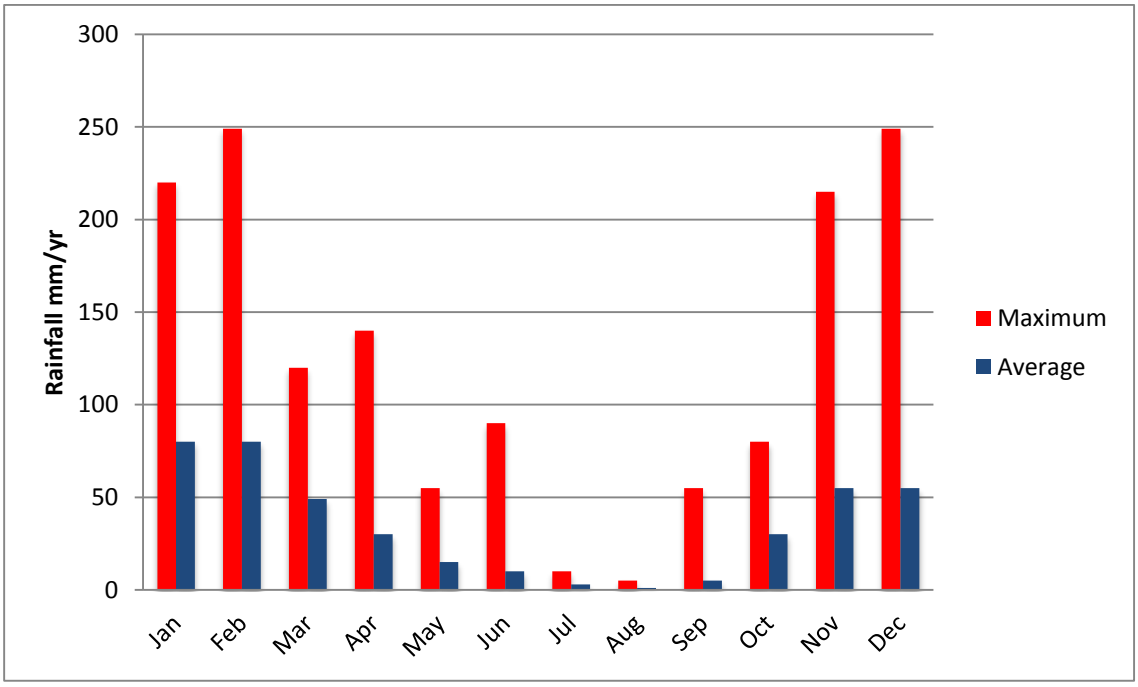


Figure 1.2 Average and maximum rainfall at Dibete (Data collected from CCC Station)

The dominant soils in the area are arenosols: sands, loamy sands and sandy loams, which are all well drained. More clayey luvisols and petric calcisols occur in the southern part of the area. Hardpan layers such as calcrete and ferricrete occur along valleys. The hardpan horizons tend to impede infiltration resulting in perched aquifers.

The main vegetation types in the area are Sandveld (Northern Kalahari Tree and Shrub Bush Savanna); Arid Sweet Bushveld (Thicket and Shrub Savanna on clay and calcrete) and Shrub Sandveld on sandy soils.

## 1.3 Geological and Hydrogeological Setting

### 1.3.1 Stratigraphy

The study area falls within the central Kalahari Karoo basin (Smith, 1984). The geology of the area is primarily dominated by the Karoo Supergroup rocks. The area is predominately covered by basalt(70%) followed by Ntane Sandstone (25%) and Kalahari sands (5%).The description and the geology map are shown in **Error! Reference source not found.** and Figure 1.4.

The Archaean basement consists of rocks of the Limpopo Mobile Belt (c.2200 Ma), which outcrops along the southern edge of the study area. The outcropping granites and migmatite form a part of the Mahalapye granite massif. The Waterberg Supergroup covers the eastern part of the study area. Only the lower members, the Mannyelanong Hill, the Lokgalo and the Masama formation outcrop in this area. The Pilanesberg dyke swarms and the Glenover dyke swarm (1300 - 900 Myr) intruded the Waterberg formation and occur immediately west of the Khurutse fault zone. These intrusions are comprised of dolerites, diorites, granodiorites and syenites (DGS, 1988).

The Karoo Supergroup culminated c. 180 Ma in the flood basalts of the Ramaselwana Volcanic Formation. The period in which the formation was extruded was relatively short,

about 10 Ma. The lavas were extruded along the axes of the main faults (Zoetfontein, Khurutshe and Makhujwane) with progressive movement (down-throw) along the faults to the north, east and south respectively (DGS, 1988).

The synchronous extrusion and down-throw results in a thick lava pile along the down-throw fault axes. Drilling results have proven > 400 m of basalt south of the Makhujwane Fault and 450 m east of the Khurutshe Fault (Figure 1.3). The Karoo Supergroup covers the western part of the study area. The occurrence of the entire Karoo sequence has been proven by drilling (Geoworld, 2010).

Table 1.1 Stratigraphy of project area (Source: Smith 1984)

| Age | Stratigraphic Unit | | | Lithology |
|---|---|---|---|---|
| | Supergroup | Group | Formation | |
| Cenozoic | | Kalahari | Kalahari Beds | Sand, calcrete and clay |
| Mesozoic | Karoo | Stormberg Basalt | Ramoselwana Volcanics | Crystalline, massive, amygdaloidal basalt |
| | | Lebung | Ntane Sandstone | Aeolian sandstone. Medium to fine-grained with minor mudstone intercalations. Partially fluvial towards the base |
| | | | Mosolotsane | Fluvial red beds. Siltstone and fine-grained sandstone |
| | | Beaufort | Tlhabala | Non-carbonaceous mudstones and siltstones with minor sandstones |
| | | Ecca | Letlhakeng | Siltstones and carbonaceous mudstones with coal |
| | | | Korotlo | Coals and coaly mudstones and sandstone |
| | | | Dibete | Coals and carbonaceous mudstones |
| | | | Mmamabula, (upper, middle, and lower) | Interceded sandstone, siltstone and carbonaceous mudstones |
| | | | Maphashalala | Post-glacial lacustrine mudstones and siltstones marking the base of the Ecca Group |
| | | Dwyka | Dukwi | Base of Karoo sequence, tillites and shales, varved siltstones and mudstones |
| Proterozoic | Waterberg | | Pilanesberg & Glenover Dyke | Dolerite dykes & sills, diorites, granodiorites and syenites |
| | | | Masama | Red arkosic sandstone, quartzites, siltstones, shale & greywacke |
| | | | Lokgalo | Red siltstone, mudstone and shales |
| | | | Mannyelanong Hill | Red sandstone and conglomerate |

| | | | | |
|---|---|---|---|---|
| Archaean | Basement | Limpopo Mobile Belt | | Granite gneiss and amphibolite |

The Dwyka Group consists of the Dukwi Formation. It is comprised of tillites, shale, varied siltstones and mudstones that were deposited in glacial and periglacial environments. The Dukwi Formation is overlain by the Ecca Group sediments that comprises largely of carbonaceous mudstones thinly interbedded with coal seams.

The Ecca Group succession within the study area includes the Maphashalala, Mmamabula, Dibete, Korotlo and Letlhakeng Formations. The Letlhakeng formation is the youngest formation in the upper Ecca and is recorded from drilling to the west of the Khurutse Fault (WSB, 2015). The Ecca Group is overlain by the Beaufort Group, which consists of the Tlhabala Formation that comprises of monotonous variegated, commonly silty or calcareous sequence of mudstones.

Overlying the Beaufort Group is the Lebung Group, which is interpreted as the beginning of a continental “Red Bed” style sedimentation of distal alluvial fans in a shallow environment under oxidizing conditions, followed by a desert environment in which aeolian sands were deposited. The group comprises of the Mosolotsane and Ntane Sandstone Formations. The Mosolotsane Formation, which is conformably overlain by Ntane Sandstone Formation (Plate 1) is formed by a sequence of white, pink and reddish brown, fine grained sandstones and siltstones often associated with some reddish mudstone intercalations. The depositional environment for this formation is inferred to as one in which fluviatile environment prevailed. The lithology of the Ntane Sandstone Formation is homogenous, consisting of fine- to medium- grained, well sorted, reddish to white massive sandstone, interpreted as being of aeolian origin. There is a downward progression to an argillaceous member comprising mudstones and siltstones. A sample from one of the drilled boreholes is inserted for visualisation of the sequence in Masama area geology (Plate 3).

Plate 1 Ntane Sandstone Outcrop

Volcanic lavas of the Stormberg Basalt Group (Plate 2) unconformably overlie the Ntane Sandstone Formation. The basalt in this area, known locally as the Ramoselwana Volcanic Formation, consists of fine grained, dark grey, black, brown and purple coloured basalt. Thick lava sequences are preserved in graben structures, the boundary faults of which were still active during eruption. The formation consists of amygdaloidal basalt flows. Overlying these basalts are the sand, gravel, and marls of the Kalahari beds that cover almost the entire study area. Their thickness decreases from west to east. Duricrusts of silcrete and mainly calcrete are very extensive in the whole area, but are probably not continuous.

Plate 2 Stormberg Basalt outcrop

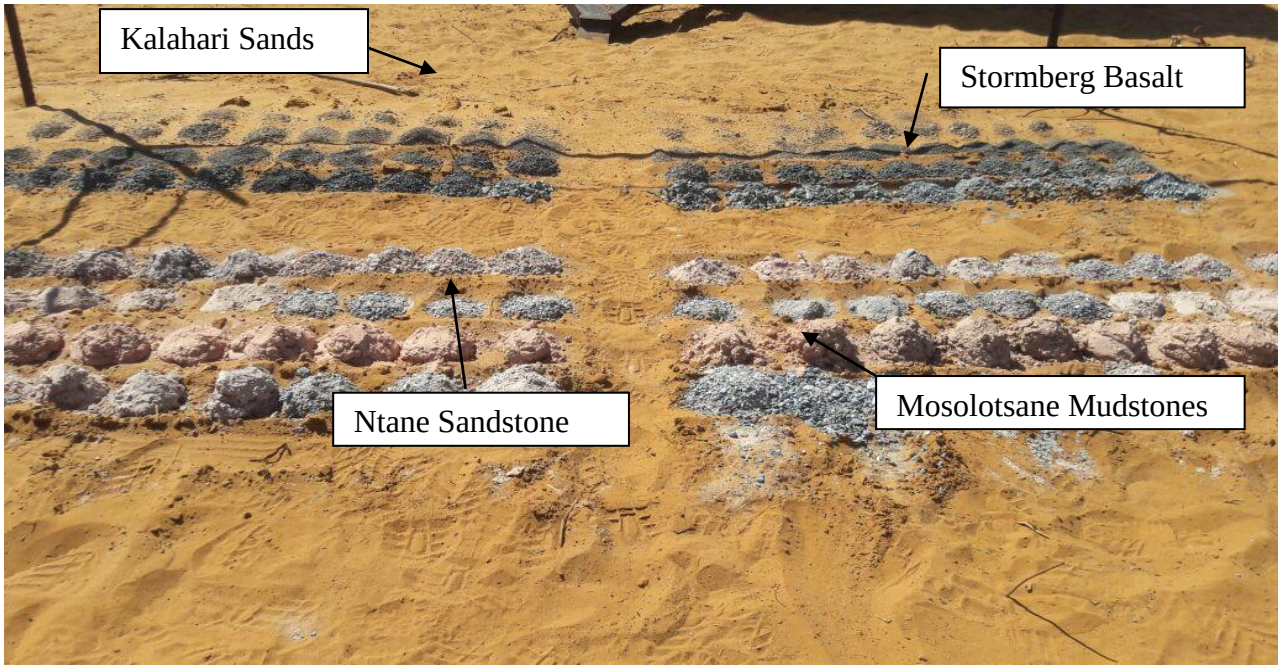


Plate 3 Photo of collected 1m interval chip samples (BH 11164)

### 1.4 Structures, Groundwater and Recharge

During the Eastern Botswana Water supply study carried by the Department of Water Affairs in 1984, the Khurutse area was identified for its groundwater potential for high yielding boreholes sited in fault zones with high permeability. The most important aquifer is the Ntane Sandstone, which is compartmentalised by block faulting where the formation has been eroded in uplifted portions. Drilling and geophysical exploration done by Geoworld (2010) shows that there is hydraulic connection along faults where they occur in juxtaposition, otherwise the faults act as barrier boundaries and a parallel relationship between the major faults with cross cuttings from other faults that exist in the area.

The regional structure is important in understanding the structure of the study area. The study area lies between and interconnects a large Karoo basin to the west, underlying most of the Kalahari. Aeromagnetic data was acquired from the Department Geological Surveys (DGS) national survey. Flight lines were extracted and filtered to produce images of Analytic Signal (Second Vertical Derivative; Figure 1.5). The objective being to map out the extent of the Stormberg Basalt and/or dolerite and to identify the main structures (faults and dykes). The interpreted data was used to produce the geology and lineament map shown in Figure 1.4. Owing to the similarity in magnetic response, differentiation between areas underlain by basalt as opposed to dolerite sill was difficult. Major faulting took place in the north-westerly direction with two major post Bushveld fault systems, the "Rustenberg Fault System" and the "Brits Fault System" (: Duplessis and Walraven, 1990; Tessema et.al 2012; Bamisaiye, 2015). These faults are very noticeable on the aeromagnetic survey.

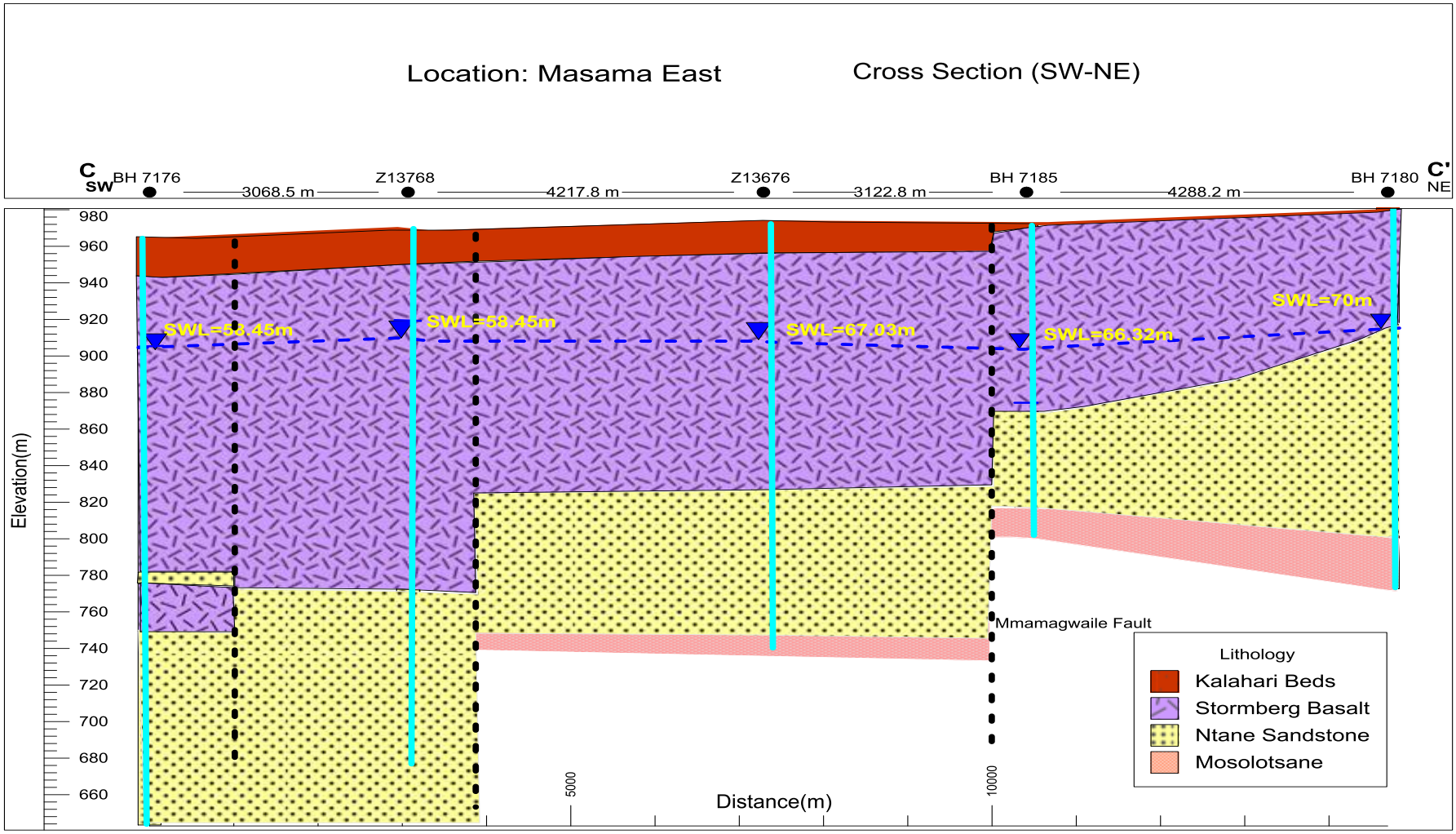


Figure 1.3 Masama geological Cross Section (SW-NE) showing direction in which the basalt thins to the NE

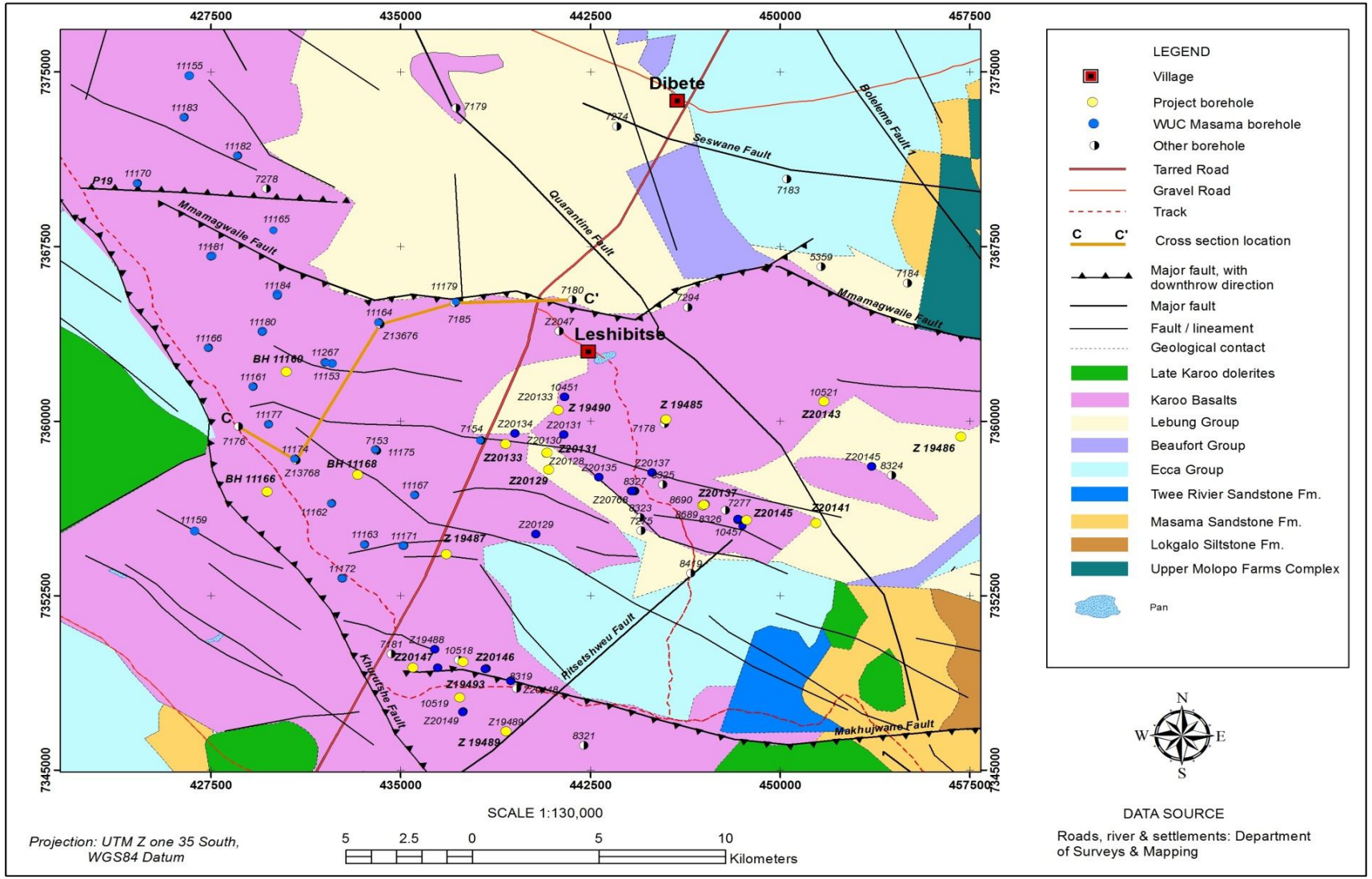


Figure 1.4 Geology and lineaments in study area

The approximately east-west trending saddle just west of Mmamabula coincides with the Zoetfontein Fault, and the northwest trending valley and escarpment just north of Mosomane coincides with the Khurutshe Fault. The Khurutshe Fault abruptly turns to the west and eventually merges with the Zoetfontein Fault near Kgomo dia Tshaba village (WSB, 2015). Comparison of geological maps with topographic data suggests that these are not the only places where topographic features and structure coincide (Keller, 1988).

In the southern part of the basin the major structures have down-throw to the north; these include the Zoetfontein and the Bokwete Faults. The Khurutshe Fault downthrows to the east and plunges to the north-west. To the east two major faults with a parallel trend to that of the Khurutshe Fault are the Boleleme 1 and Boleleme 2 Faults. The Makhujwane Fault has a similar 400 m displacement in the basalt from north to south across the fault downthrowing to the south (Figure 1.4).

The Mmamagwaile Fault does not have a strong aeromagnetic expression and marks the geological contact between the basalt in the south and unconfined Ntane Sandstone aquifer to the north i.e. southerly downthrow. The fault strikes westwards from Nokana settlement for approximately 10 km before swinging northwest eventually truncating at the P19 Fault. There are numerous other smaller structures with a West North West (WNW) - East South East (ESE) trend which essentially break up the area into vertically displaced blocks (Figure 1.4 and Figure 1.3).

Recharge in the area is believed to be occurring in the region west of Dibete village where the area lies at the highest elevation of 1040 m.a.s.l. with a corresponding piezometric mound (Figure 1.6). Groundwater flow is towards the southeast with a discharge towards the Notwane

River channel which has an elevation of 900 masl. Some areas, especially in the eastern region of the study area where Ntane Sandstone sub-crops are also thought to be areas of recharge.

Analysis of aquifer test data using the program TESTCURVE 9.4 in numerous boreholes drilled and tested in the area has shown that the Ntane Sandstone aquifer transmissivity (T) and storativity(S) are highly variable with mean values of 154 $m^2$/day and 0.009, respectively (WSB, 2015a). Table 1.2 shows the calculated transmissivity, storativity and hydraulic conductivity (K) for the selected project boreholes using TESTCURVE 9.4.

Table 1.2 Calculated aquifer parameters for the sampled boreholes

| **Borehole ID** | **location** | **Year** | **Aquifer Thickness** | **Transmissivity** | **Storativity** | **Hydraulic Conductivity** |
|---|---|---|---|---|---|---|
| | | | **(m)** | **$m^2$/day** | | **m/day** |
| BH11160 | masama west | 2017 | 123 | 115 | $5.4 * 10^{-3}$ | 0.93 |
| BH11168 | masama west | 2017 | 142 | 83 | $2.0 * 10^{-3}$ | 0.58 |
| Z19485 | masama east | 2014 | 100 | 155 | $8.0 * 10^{-2}$ | 1.55 |
| Z19486 | masama east | 2014 | 133 | 50 | $2.5 * 10^{-2}$ | 0.38 |
| Z19487 | masama east | 2014 | 116 | 115 | $4.0 * 10^{-2}$ | 0.99 |
| Z19489 | masama east | 2014 | 142 | 33 | $1.0 * 10^{-2}$ | 0.23 |
| Z19490 | masama east | 2014 | 133 | 720 | $1.0 * 10^{-2}$ | 5.41 |
| Z19493 | masama east | 2014 | 108 | 32 | $1.0 * 10^{-2}$ | 0.30 |
| Z20129 | masama east | 2015 | 137 | 7 | $1.7 * 10^{-2}$ | 0.05 |
| Z20131 | masama east | 2015 | 148 | 36 | $3.9*10^{-5}$ | 0.24 |
| Z20133 | masama east | 2015 | 169 | 53 | $3.1 * 10^{-5}$ | 0.31 |
| Z20137 | masama east | 2015 | 219 | 25 | $1.3 * 10^{-4}$ | 0.11 |
| Z20138 | masama east | 2015 | 156 | 1022 | $6.2 * 10^{-6}$ | 6.55 |
| Z20141 | masama east | 2015 | 172 | 827 | $3.8 * 10^{-6}$ | 4.81 |
| Z20143 | masama east | 2015 | 180 | 81 | $1.9 * 10^{-4}$ | 0.45 |
| Z20145 | masama east | 2015 | 92 | 1052 | $1.5 * 10^{-4}$ | 11.43 |
| Z20146 | masama east | 2015 | 118 | 36 | $1.3 * 10^{-4}$ | 0.30 |
| Z20147 | masama east | 2015 | 134 | 32 | $3.0 * 10^{-5}$ | 0.24 |
| Z20148 | masama east | 2015 | 129 | 55 | $1.1 * 10^{-5}$ | 0.43 |

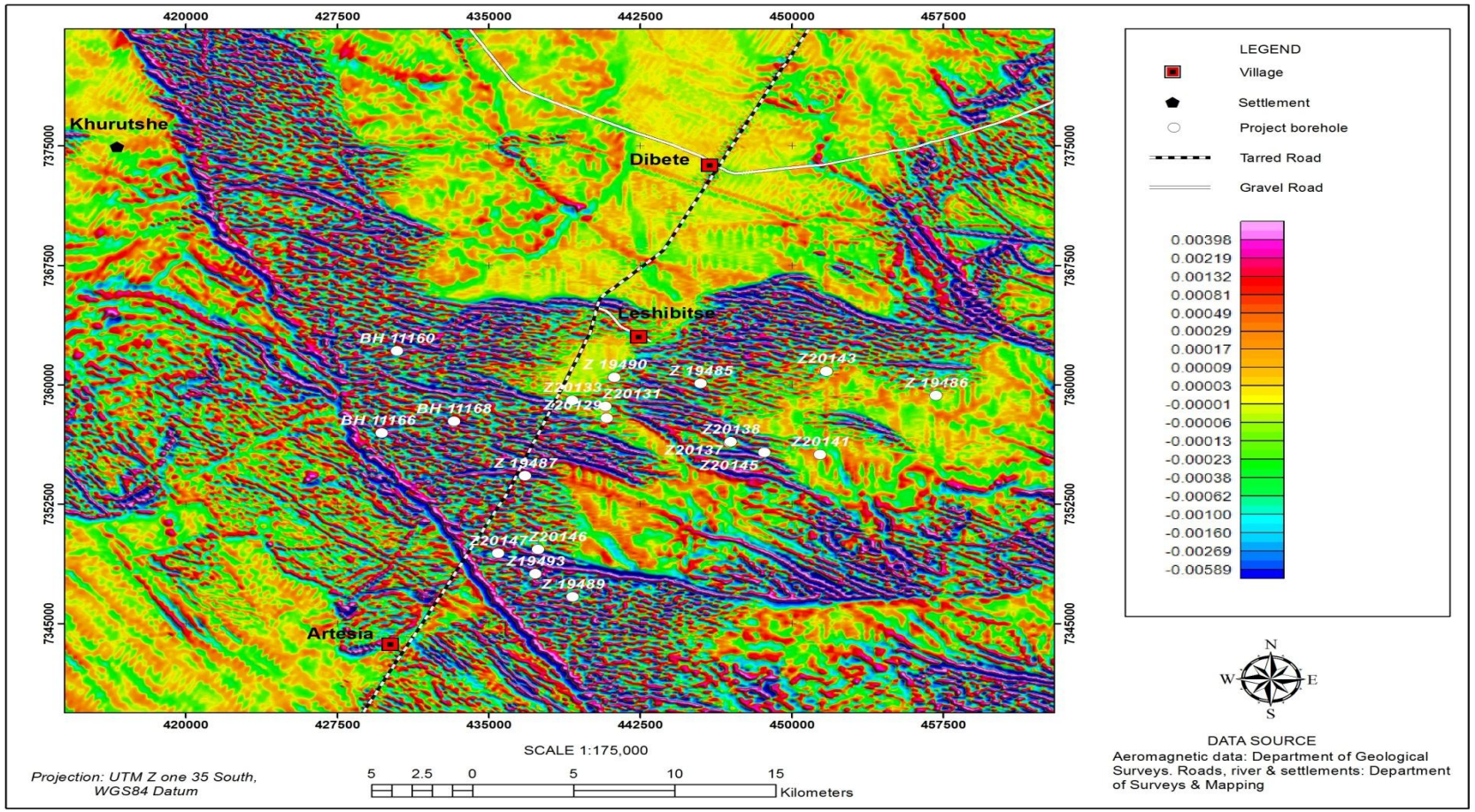


Figure 1.5 Second vertical derivative aeromagnetic map of the study area (Legend in nanoTesla, nT).

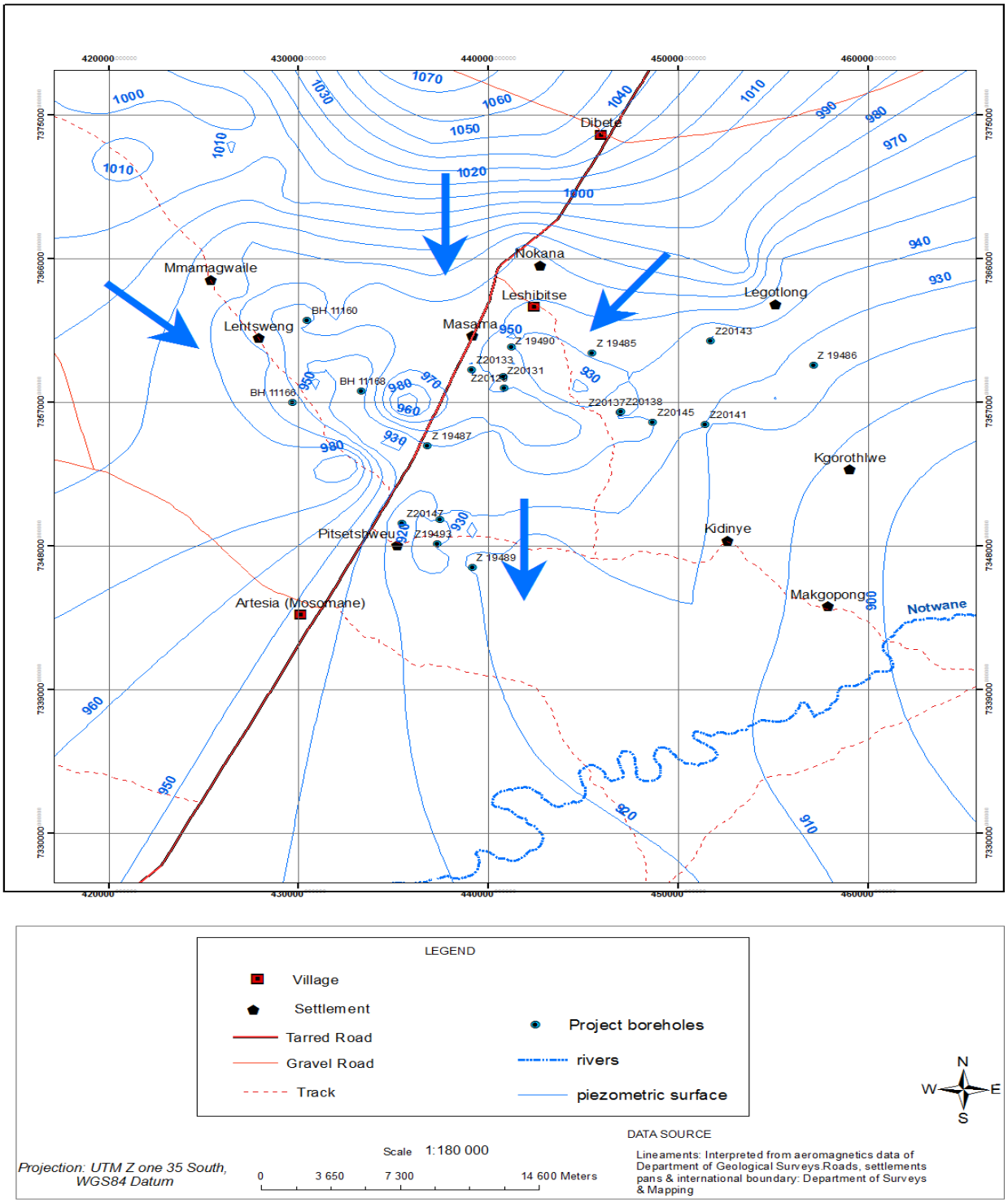


Figure 1.6 Piezometric surface map

## 1.5 Chemical and Isotopic Species in Groundwater

### 1.5.1 Chemical Species in Groundwater

Stability and movement of chemicals or isotopes through the subsurface is adversely affected by various physico-chemical processes. These processes may occur in the unsaturated or saturated zone depending on the prevailing groundwater compositions and water levels. In addition to secondary (physical) processes such as hydrodynamic dispersion, the substance may react with other mineral species or solid phase, or undergo biological transformation or even decompose due to radioactive decay. Based on the water –rock ratios during these times of active reactions, these processes can occur simultaneously and some minerals or isotopes can be saturated or undersaturated with respect to the initial water composition.

Unlike studies investigating groundwater pollution, where the main concern is to trace the migration pathway for contaminants, here the fate is to map the behaviour and shift of environmental species (chemicals and isotopes) from natural system conditions.

The concentration of a certain dissolved species in groundwater is what categories it as major, minor or trace. These three categories are widely used in a numerous branches of analytical science and the terminologies were employed by Hem (1985), where it was stated that any dissolved species with a concentration measuring greater than 5 mg/l is classified as a major constituent. On the other hand, a minor constituent was classified as having a range of 0.1-5 mg/l. The last category, trace constituents, was assigned to species having concentrations below 0.1 mg/l.

Most dissolved species are either negatively or positively charged with the exception of some such as silica. Positively charged ions (cation) in groundwater with emphasis to the major constituents are Sodium Potassium ($K^+$), Calcium ($Ca^{2+}$) and Magnesium ($Mg^{2+}$). Major

negatively charged ion, anions, include: Chloride ($Cl^-$) Fluoride ( $F^-$) Bicarbonate ($HCO^-_3$) , carbonate ($CO^{2-}_3$) , Nitrate ($NO^-_3$) and sulphate ($SO^{-2}_4$).

Dissolved gases can also play an important part in investigating an aquifer. However, because of their instability they are better done during field sampling. Some of the important gases are hydrogen sulphide ($H_2S$) and dissolved oxygen (DO). Literature on these can be found in works of authors such as Mazor (1972), Phillip (1981) and numerous others

The Kalahari aquifers have been described by Smith (1984) and Carney and Aldiss (1994) and they are categorised into two geochemical and hydrological classes:

(1) those overlain by non or semi-permeable, low permeability layers and open to exchange with atmosphere, this is identified as and aquitard, and:

(2) those overlain and underlain by impermeable layers and closed to any form of exchange with the atmosphere ,referred to as confined aquifers.

The Masama Sandstone aquifer falls under the second category, where it is unconformably overlain by basalts and conformably underlain by mudstones. This arrangement makes it less likely for any potential recharge to reach this aquifer directly unless through conduits such as fractures and faults. Since this movement is rather occurring via such structures, groundwater tends to dissolve and incorporate chemical species on its way down, owing to difference in pH, temperatures and the ever evolving groundwater composition attained down-gradient. Alongside this entrapment of chemical species is the absence of dissolved oxygen at depth, which does not favour some of the mineral that would have been brought along, for such their stability tend to be compromised and they are either, transformed, absorbed or exchange for others ( Domenico and Schwartz, 1990).

### 1.5.2 Factors Controlling the Chemistry of Groundwater

Natural water chemistry is forever evolving during its travel in the hydrological cycle. Various processes fractionate and change the composition of the water just from the time it rains to the time it hit the ground and percolates or infiltrate into the ground. In general, the rain composition is controlled by the type and concentration of atmospheric particulate matters (Ward and Robinson, 2000). Factors such as temperature, time of day or year, cloud cover, humidity, altitude and latitude also play a role in the type of precipitation that will occur. The chemistry of rain was determined from various environments and found to be slightly acidic (pH 4.5-6.5), very dilute and oxidizing (Freeze and cherry, 1979; Hem, 1985).

In the saturated and unsaturated zone, the rain water reacts with the various sediments in different ways depending on the rock type, presence of organic matter and also how long it sits or sinks in the particular area. First the salinity of water is increased by leaching process in the unsaturated zone as this is the zone.

If there is positive infiltration (recharge), the infiltration rate will be inversely proportional to the increase in salinity (Mazor, 1982; 1985). Conversely, if a considerable amount of water is evaporated , encrustation will occur and the dissolved constituents will re-dissolve in the next rain event, altering the composition of the rain, and thus the water reaching the water table will have high total dissolved solids compared to water that underwent direct infiltration.

The abundance of roots and the openness for gas exchange and diffusion in this soil certifies its lower pH level (acidic) compared to the saturated zone. Freeze and cherry, (1979) deduced an empirical formula (Equation 1) to account for the reactions that cause such high pH level. This equation works with respect to the reversible chemical reaction that occurs between rain water ($H_2O$) and carbon dioxide ($CO_2$), where the two react to form carbonic acid ($H_2CO_3$), a weak acid.

The source of the $CO_2$ is the decomposition of organic matter and respiration in plants. Humic acid also contribute to the acidity in the soil. All these processes reduce the content in the soil giving leeway for anaerobic reaction such as reduction of nitration and sulphates to occur, and they too serve as sources for $CO_2$ (Mazor et al., 1980). Combination of all these $CO_2$ being produced, in-turn decrease the pH of water and raises partial pressure of $CO_2$ ($PCO_2 = 10^{-3}$ to $10^{-1}$ bar) to amount higher that atmospheric value. At this pH value, 4.5, with partial pressures of $10^{-1}$ bar and a standard temperature (25°C), dissolution of some minerals occurs. Examples of common reaction that are affected by the reduced pH are those involving calcite and albite.

$$H_2O + CO_2 \leftrightarrow H_2CO_3 \qquad (1)$$

$$CaCO_3 + H_2CO_3 = Ca^{+2} + 2HCO_3^- \qquad (2)$$

$$\underset{\text{(Albite )}}{NaAlSi_3O_{8(S)}} + H_2CO_3 + 9/2H_2O = Na + HCO_3^- + 2H_4SiO_4 + 1/2\ \underset{\text{(Kaolinite)}}{Al_2Si_2O_5(OH)_{4\,(s)}} \qquad (3)$$

As seen in the above chemical reaction, calcite dissolves to form only dissolve species while albite forms both amorphous solid and dissolved species. The terms used for such are congruent and incongruent, respectively. These reactions continue to occur, for as long as there is supply of new water to the unsaturated zone and production of carbon dioxide. Freeze and Cherry (1979) described that, even though there are other reactions that also increase acidity, such as oxidation of iron and sulphur present in the soils, their role is insignificant in most cases. Once infiltrated water reached the saturated zone, processes involved are controlled by the geologic material they come in contact with. In this zone the hydraulic properties of the geologic material and flow system also play an important role.

The ease at which the water moves and the time it take being in contact with this materials (residence time) can determine how much of the dissolvable material is incorporated into the

solution. This natural tendency for groundwater total dissolve solids to evolve from low to high concentration as it moves downgradient is discussed in a paper by Chebotarev (1955), where he concludes by proposing a sequence in which the evolution occurs as shown below, with trend moving from left to right.

$$HCO_3^- \rightarrow HCO_3^- + SO_4^{2-} \rightarrow SO_4^{2-} + HCO_3^- \rightarrow SO_4^{2-} + Cl^- \rightarrow Cl^- + SO_4^{2-} \rightarrow Cl^-$$

Some of the primary factors for the evolution of the groundwater amongst others are temperature and pressure. The stability and availability of most chemical constituents is affected by these physical parameters (Ward and Robinson, 2000). The order in which the chemical constituents are incorporated is also vital, as an example, water bearing magnesium, divalent ions, would be exchanged for monovalent ions such as sodium.

## 1.6 Groundwater Isotopes

This section discusses isotope in groundwater with more emphasis on those chosen for use in the study. Many naturally stable and radioactive isotopes exist in the atmosphere but for the purpose of this study, environmental isotopes of Oxygen-18($^{18}O$) , Deuterium ( $^{2}H$), Tritium ( $^{3}H$) and radiocarbon ($^{14}C$) were chosen mainly because of their ability to distinguish between recent and fossil water which is facilitated by their different half-lives. Radiocarbon was used to assist in determining whether the groundwater in the study area is of paleo-origin whilst tritium was used to detect any input of recent rain activities. The $O^{18}$ and $^{2}H$ assisted in determining the environmental processes that the rain water encountered prior to infiltration and afterwards.

### 1.6.1 Environmental Stable Isotopes

The difference in atomic mass of a particular element is significant when it comes to isotope. These differences cause the same element to have different atomic masses and for that cause

fractionation in isotopes of lighter elements (Fritz and Fonte, 1980). Stable isotope results are expressed in δ units, defines as

$$\delta\ (‰) = 1000\ (R\text{-}R_{st})/R_{st}$$

where $R_{st}$ and R are isotopic ratios of the standard used and measured sample, respectively. The reference used for stable isotope ($^{18}O$ and $^{2}H$) is the Vienna Standard Mean Ocean Water (VSMOW). Craig (1961) reported the linear correlation between $^{18}O$ and $^{2}H$ after an extensive collection and analyses of precipitation from various locations, which is identified as Global Meteoric Water Line. The regression line is expresses as

$$\delta^{2}H = 8*\delta^{18}O + 10\ (‰)$$

The line has a slope of 8 as a reference and differs from region to region depending on the distance from the sea. The GMWL provides reference for interpretation of groundwater provenance. The key observation from Craig‘s research was that waters in cold regions were isotopically depleted while warmer regions waters were enriched. This partitioning was later recognised as a tool for characterising groundwater recharge environment and has since been used in groundwater provenance studies.

Dansgaard (1964) further used this linear relation but with a new variable added. He demonstrated that $\delta^{18}O$ and temperature were dependent, as such reason why fractionation increases with decreasing temperatures. This dependence of isotopic content on temperature has been used by hydrogeologists to estimate (Fritz and Fonte, 1980):

(1) Recharge area altitude and recharge amount by linearly relating the precipitation isotopic content and the amount of rain based on the negative correlation

(2) Paleo-temperatures based on that isotopically depleted waters are formed when precipitation falls under cool climate conditions

Temperature effect thereby testifies why the $^{18}O$ and $^{2}H$ content of continental precipitations is more depleted than coastal or marine precipitation. Consequently, why summer rains are more depleted with respect to winter rains (Boronina, 2005).

Rain-out processes from clouds, partial evaporation of rain drops and isotope exchange cause isotopically depleted precipitation. Verhagen (1990) related the isotopic composition of rain water collected from period where there were heavy rains to the amount of precipitation and concluded that an inverse relationship exists. Rain-out processes from clouds, partial evaporation of rain drops and isotope exchange cause isotopically depleted precipitation. Verhagen (1990) related the isotopic composition of rain water collected from the period where there were heavy rains to the amount of precipitation and concluded that an inverse relationship exists. Beekman et al. (1997) also used the same principle in an isotope study in Letlhakeng-Botlhapatlou and in the Central Kalahari where he also confirmed the inverse relation from the Lobatse and Malwelwe stations data in Botswana.

### 1.6.2 Radionuclides of Atmospheric Origin

Radiocarbon and tritium are regarded as radionuclide of atmospheric origin resulting from cosmic rays spallation. A large number of applications and review on these radioisotopes has been conducted (Wallick, 1973; Davis, 1978; Freeze and Cherry, 1979). The fundamental assumptions are that the radionuclides concentration has been stable for quite some time prior to the spikes experienced in 1950's. Mook (1980) proposed the half-lives for carbon-14 and tritium to be 5730 years and 12.34 years, respectively with initial atmospheric concentrations of 3.6 Tritium Units (TU) and 100 percent modern carbon (pmc).

Tritium with a half live of 12.34 years has mostly been used to date “young” groundwater. Factors affecting tritium concentration in precipitation include and not limited to atmospheric circulation patterns, coast-to-land distance and evaporation. These factors and others not stated make it difficult to clearly define the initial tritium concentration at recharge, and for that the age calculate from tritium is mostly interpreted qualitatively (Clark and Fritz, 1997).

These factors and others that are not stated make it difficult to clearly define the initial tritium concentration at recharge, and for that the age calculate from tritium is mostly interpreted qualitatively (Clark and Fritz, 1997). Groundwater containing tritium units < 0.8 TU is thought to be submodern (recharged prior to 1952), anything between 0.8 - 4 TU is a mixture of submodern and recent recharged with the present tritium concentration in precipitation assumed to be 5 TU.

Radiocarbon is largely used to date “old” groundwater, usually referred to as palaeo- and fossil groundwater. This is favoured by its long half-life of 5730 years. Like stable isotopes; $^{14}C$ has various processes that inhibit its quantification. The measurement of $^{14}C$ either as dissolved inorganic carbon (DIC) or dissolved organic carbon (DOC) also has its pitfalls. The biological transformation of organic and inorganic materials tends to add “dead” carbon into the system. To deal with this, a universal correcting and normalising of $^{14}C$ with $\delta\ ^{13}C$ is usually employed. This involves normalizing of the $^{14}C$ activities to a common $\delta\ ^{13}C$ value of -25 ‰ but bearing in mind that oxalic acid has a $\delta\ ^{13}C$ of 19.3 ‰ (Craig, 1961) therefore the fractionation of $^{14}C$ will be slightly twice that of $^{13}C$. This makes the enrichment amount to:

$$2.3(\delta\ ^{13}C_{sample} + 25)\ ‰$$

Concentration levels of $^{14}C$ are based on measurements of its half-life decay. Like every method, assumptions are made with the first being that the background concentration of the

parent nuclide is known and has been constant in the past. Secondly, the system is assumed to be closed to any subsequent losses or gains of the parent nuclide, with the exception of radioactive decay. The radioactive decay which is a measure of the stability of the radionuclide is represented by a decay equation:

$$a_{t=a_0} * e^{-\lambda t}$$

*Where* $a_0$ *= initial activity of the parent nuclide*

$a_t$ *= initial activity of the parent nuclide after some time, t*

$\lambda = decay\ constant\ and\ is\ equal\ to \frac{ln2}{t1/2}$

Studies of $^{14}C$ value have shown that it can be used as evidence for recharge occurrence, with values of about 100 pmc being classified as recharge of approximately 100 years prior to 1950's while those with values significantly above 100 pmc are assumed to be waters recharged after 1950's (Verhagen et.al., 1974, Tamers, 1975)

# 2 MULTIVARIATE STATISTICAL ANALYSIS OF HYDROCHEMICAL DATA

With the increasing demand for groundwater as a complementary source of water for the Gaborone and its neighbouring villages, extensive geochemical programs have been carried out on the Masama Sandstone aquifer. Although isotopes have not been employed much due to the cost and lack of availability of an institution for such analysis in Botswana, a lot of hydrochemical data has been collected on the Masama Sandstone aquifer from individual boreholes since the early 1990's. It is for this reason that multivariate statistical technique/statistical data analysis techniques (SDAT) can serve as a good alternative to the traditional data mining methods.

A vast amount of physico-chemical parameters are normally measured per borehole and for that it is not uncommon for a single borehole to have close to 10 or 15 parameters spatially distributed in space and time. The important thing is how well can this data be put in use to understand the aquifer. Some of the variables are alkalinity, total dissolved solids, temperature, electrical conductivity and major chemical constituents, and a detailed explanation of these is covered in the previous Chapter 1. The expectation is that these variable should somehow cross-correlate with one another as their distribution in space and time is usually correlated because of the chemical processes they transition through.

The widely used traditional methods for the interpretation of hydrochemical and isotopic data has been qualitative graphical data representations, through the use of histograms, scatter plots, piper, schoeller, radial and stiff diagrams. The most popular of these plots is the piper diagram, which has in many encounters succeeded in classification of groundwater. The main short fall is its inability to use/involve other chemical constituents outside of the prefixed selections and failure to identify geochemical processes involved in groundwater evolution.

## 2.1 Description of Multivariate Statistical Analysis Techniques

Multivariate statistical techniques use algorithms to solve problems at hand. Data sets are turned and viewed in both two dimensions (2D) and three dimensions (3D) to eliminate possibilities for a suppressed variable that might be overlooked by simple linear statistics (Dalton and Upchurch, 1978). Suppose we represent an aquifer, X, with P x N matrix, where P is the number of samples/observations with N variables, of which could be hydrological value, activity of groundwater isotope or chemical constituents concentrations with an entry $X_{ij}$ . The i and j of the X, represents i-th variable at the j-th location. This matrix can further be broken in terms of columns where Xi as X= (x1, x2, x3,.....,xn) while xj is a descriptive of the j-th location and contains values at that location. The columns of X and i-th row of X can be represented as P-dimensional and N-dimensional space, such that X becomes a cloud of P-points in this space. In these clouds, it becomes much simpler to measure and see the principal direction of spread of variables and individually pick the variables that cause the most spread. The overall objective of SDAT is to simplify interpretation by finding a set of q ($q < p$) new variable that are usually unobservable by other methods.

### 2.1.1 Principal Component Analysis

Principal Component Analysis (PCA) shift from the usual Cartesian coordinates by introduction of a new set of orthogonal Cartesian coordinates to attain maximum variance (spread of points) from the original variable along all linear combination possible (Davis, 2002). Principal Component Analysis (PCA) shift from the usual Cartesian coordinates by introduction of a new set of orthogonal Cartesian coordinates to attain maximum variance (spread of points) from the original variable along all linear combination possible (Davis, 2002; Subyani and Al Ahmadi,2010). The first component, projection of -N points, usually represents most of the variance with regard to all possible coordinates, followed by the

second component, which its maximum variable is with regard to it being orthogonal to the first component, and so on.

### 2.1.2 Hierarchical Cluster Analysis

In contrast to conventional trilinear diagrams, hierarchical cluster analysis (HCA) does not constrain the number of variables to be used; it expresses each variable X, as a linear combination of common and unique factors. Hierarchical Cluster analysis is a statistical technique that classifies similar observed data into clusters on their dominance order (Lawrence and Upchurch, 1982; Winter et al., 2000). It ensures that the nearby points end up in the same cluster. The iteration process will always give a new cluster less 1 meaning that if there are N numbers of observations, the new formed cluster will be N-1. Each cluster contains a data point $C_i = X_i$, a pair of clusters that is closet, min D ($c_i$. $c_j$) is sought. The clusters ci and cj are merged into a new cluster $c_{i+j}$ and the old $c_i$ and $c_j$ is removed from the collection C. The Euclidean distance measured is between clusters and not points. At the end of the iteration process a dendrogram is produced, that is a hierarchical tree representing the clusters. For computing the proximity between observations, the technique uses dissimilarities and euclidean distance.

# 3 MATERIALS AND METHODS

A total of 20 boreholes that best represent the Masama sandstone aquifer were sampled. The criterion used was to select boreholes along the flow path and on both sides of the major structural faults to be able to see the extent of influence on the aquifer response and connectivity. Due to other constraining factors such unavailability of pumps in other newly drilled boreholes isotopes tests were restricted mostly to the existing boreholes. The total analyses number for different tests varies due to such reasons and some boreholes will be discarded for quality control.

The location of the sampled boreholes is shown as **Error! Reference source not found.** and Table 3.1 lists the available data for the selected boreholes with respect to their location and geographical position. Detailed lithological and borehole construction details is attached as Appendix A. Surface elevations and coordinates were collected using a handheld Geographical Point System (GPS) while water levels recorded were compiled from Water Surveys Botswana (2015/2016) drilling report.

## 3.1 Field Procedures

Prior to sampling, the boreholes were purged for 2-3 minutes and sample bottles pre –washed at least twice with water from the borehole. Two samples per borehole were collected for chemical analysis in 1 Litre (L) polythene plastic bottles and filled to the brim to reduce any potential for oxidation. The other sample was acidified with 1 M nitric acid for preservation of cation while the other was left un-acidified. Tritium samples were also collected in 1 L polythene plastic bottles. For stable isotope analysis water samples were collected in 10 ml glass bottles and stored in a cooler box with temperature maintain at around 4 degree Celsius (°C).

Table 3.1 Characteristics of the sampled boreholes

| Borehole No | Latitude | Longitude | Location | Borehole depth (m) | Surface Elevation (m .a .s .l) | Depth to Water (m) | Water Table Elevation (m .a .s .l) |
|---|---|---|---|---|---|---|---|
| Z20146 | 437458 | 7349643 | Makhujwane | 252 | 920 | 42 | 878.0 |
| Z11160 | 430467 | 7362107 | Masama West | 247 | 951 | 60.6 | 890.4 |
| Z20145 | 453626 | 7358053 | Masama East | 155 | 935 | 44.8 | 890.2 |
| Z19486 | 484520 | 7350977 | Masama East | 149 | 917 | 33.3 | 883.7 |
| Z20129 | 440343 | 7355131 | Masama East | 176 | 951 | 54.6 | 896.4 |
| Z19489 | 439163 | 7346635 | Makhujwane | 436 | 908 | 54 | 854.0 |
| Z20147 | 435463 | 7349386 | Makhujwane | 339 | 934 | 46.2 | 887.8 |
| Z19490 | 441220 | 7360468 | Masama East | 161 | 930 | 58 | 872.0 |
| Z20131 | 441452 | 7359414 | Masama East | 214 | 952 | 63.3 | 888.7 |
| Z20143 | 451729 | 7360828 | Masama East | 201 | 927 | 49 | 878.0 |
| Z19485 | 445446 | 7360347 | Masama East | 184 | 926 | 49 | 877.0 |
| Z11166 | 427392 | 7363146 | Masama West | 347 | 944 | 53.4 | 890.6 |
| Z20137 | 444119 | 7356983 | Masama East | 237 | 944 | 49 | 895.0 |
| Z20133 | 441489 | 7361040 | Masama East | 210 | 956 | 62.3 | 893.7 |
| Z20141 | 451410 | 7355610 | Masama East | 181 | 938 | 44 | 894.0 |
| Z20138 | 446996 | 7356387 | Masama East | 180 | 926 | 51.65 | 874.4 |
| Z19487 | 486718 | 7354828 | Makhujwane | 234 | 917 | 47 | 870.0 |
| Z11168 | 7357684 | 433289 | Masama West | 286 | 937 | 59 | 878.0 |
| Z20144 | 7355730 | 448663 | Masama East | 194 | 945 | 51.6 | 893.4 |

*Coordinates recorded in UTM Zone 35S , WGS84

Radiocarbon samples were collected in 50 L jerry cane. Reagents added were Sodium hydro-oxide was added to raise the pH into alkaline range and Barium Chloride to precipitate Barium Carbonate ($BaCO_3$). Phenolphthalein was used to attain the right pH. The solution was left over night and the precipitate $BaCO_3$ collected in one litre plastic bottles. Physico-chemical parameter including temperature, Total Dissolved Solids (TDS) and Electrical conductivity (EC) were measured with a Hanna handheld TDS-pH meter.

## 3.2 Laboratory Procedures

### 3.2.1 Chemical Analysis

The samples for the cations were acidified with 1 M Nitric acid before storage. Analysis for cation, anions and alkalinity was done at the Water Utilities Corporation Hydrogeology Laboratory. Time for analysis of sample upon arrival, was done within 48hrs for the Nitrite and Nitrate and one week for other ions. Ion Chromatography (Dionex- ICS 3000) was used to analyse the anions and Induced Coupled Plasma Optical Emission Spectrometer (ICP-OES) for the cations, Total Alkalinity, Calcium Hardness and pH were analysed through titration by Autotitra T70 machine.

### 3.2.2 Isotopic Analysis

The stable isotopes of $\delta^{2}H$ and $\delta^{18}O$ were analysed by using the Liquid Water Isotope Analyzer-model 45-EP at the University of the Witwatersrand, South Africa. The instrument contains the laser analysis system and an internal computer, liquid auto-sampler, a small membrane vacuum pump, and a room air intake line that passes air through a Drierite column for moisture removal. A Hamilton micro-litre syringe was used to inject 0.75 µL of sample through a PTFE septum in the auto-sampler. The injection port of the auto-sampler is heated at 46°C to help vaporise the sample under vacuum immediately upon injection. The vapour then travels down the transfer line into the pre-evacuated mirrored chamber for analysis. A 1 ml aliquot of a sample was pipetted into a 2 ml auto-sampler glass vial and closed with PTEF septum caps. Five standards were used in the analysis procedure where the laser machine automatically calibrates itself and measure stable isotope values. The standards used are 5C: $\delta^{2}H$ -9.2 ±0.5, $\delta^{18}O$ -2.69 ±0.15, 4C: $\delta^{2}H$ -51.6 ±0.5, $\delta^{18}O$ -7.19 ±0.15, 3C: $\delta^{2}H$ -97.3 ±0.5, $\delta^{18}O$ -13.39 ±0.15, 2C: $\delta^{2}H$ -123.7 ±0.5, $\delta^{18}O$ -16.24 ±0.15, 1C: $\delta^{2}H$ -154 ±0.5, $\delta^{18}O$ -19.49 ±0.15. The laser machine is capable of providing accurate results with a precision of

approximately 1 permil (‰) for $\delta^{2}H$ and 0.2‰ for $\delta^{18}O$ in liquid water samples of up to atleast 1000mg/l dissolved salt concentration.

All radiogenic isotopes analysis was conducted at iThemba Laboratory. For Tritium analysis, 20 samples were taken in 1 L PVC bottles and analysed at iThemba Labs, Gauteng, Johannesburg. The samples were distilled and subsequently enriched through electrolysis processes. 500 ml of the water sample, having first been distilled and containing sodium hydroxide, was introduced into the cell. A direct current of 10 - 20 amperes was then passed through the cell, which was cooled because of the heat generation. After a week, the electrolyte volume was reduced to 20 ml. The volume reduction of 25 times produced corresponding tritium enrichment factor of about 20. Samples of standard known tritium concentrations (spikes) were run in one cell of each batch to check on the enrichment attained. For liquid scintillation counting, samples were prepared by direct distillation of the enriched water sample from the highly concentrated electrolyte. 10 ml of the distilled water sample was mixed with 11 ml of Ultima Gold and placed in a vial in the analyser and counted 2 to 3 cycles of 4 hours. Detection limits used were 0.2 TU for enriched samples.

Another radiogenic isotope that was analysed at iThemba Laboratory was Carbon-14 ($^{14}C$). $^{14}C$ is measured in “percent modern carbon” (pmc). The activity is referenced to 95% of the Oxalic acid standard for the $^{14}C$ activity of 1950. Atmospheric $^{14}CO_2$ reacts /mixes with living biomass in living organism by the process of photosynthesis. In water bodies, $CO_2$ exchange is occurring and carbonates formed usually retain the $^{14}C$ in their molecular structures. In soil, the radiocarbon can be dissolved in solution as dissolved inorganic Carbon (DIC) or dissolved organic carbon (DOC). Apparent age or circulation of groundwater can be estimated through the use of tritium and radiocarbon.

### 3.3 Softwares

Various softwares were employed to better understand the geochemical processes governing the chemical composition of groundwater in the Masama aquifer and represent them geospatially. ArcGIS 10.3.1 and Surfer 11 were used to produce location map and contour maps for the distribution of measured chemical and isotopic constituents while graphical representations where done using piper plots in AquaCHEM.

Moreover further analyses of the results are captured with XLSTAT a statistical software that deals with information on an iteration process to reduce data to a more comprehensive and manageable quantity through establishment of similarities and relationships between observations of large data sets without losing much of information. Data analysis methods chosen from this package are Hierarchical Cluster Analysis and Principal component analysis.

# 4 RESULTS AND DISCUSSIONS

## 4.1 Hydrochemistry

Chemical data for the groundwater samples are presented in Table 4.1. Charge balance for the results was calculated using AquaChem v 5.1 software package (Schlumberger Water Services). Charge imbalances of ±10 % were taken to be laboratory analytical error. This great error decreases confidence in the data.

Complementary geochemical and isotope data show that one dominant water type is found in Masama basin. The Calcium-magnesium-bicarbonate (Ca-Mg-$HCO_3^-$) water has low salinity and is varyingly either isotopically enriched or depleted depending on the host aquifer. A trend in the $Mg^{2+}$ concentration was noticed as the basalt thickness increases. Groundwater samples collected in areas where the basalt is thick have major cation in the order $Ca^{2+}$ > $Mg^{2+}$ > $Na^+$. The groundwaters are characterized by low TDS (less than 540 mg/l).

In semi-arid regions groundwater chemical evolution is related to waters of this type (Plummer et.al., 1990; Sami, 1992: De Vries et al., 2000; Edmunds and Smedley, 2000), that are considered as recharge area waters still at the verge of evolving ( i.e early stages of geochemical evolution). Similar characteristics are also found in rapidly circulating groundwater where water rock interaction is low.

The Ca-Na-$HCO_3$ water also has TDS < 500 mg/l with an exception of one sample that has TDS= 540 mg/l and is situated in an area where basalt is absent. The sample contains almost 1:1 ratio of $Ca^{2+}$ and $Na^{+}$. The dominant cation species are $Ca^{2+}$ > $Na^+$ > $Mg^{2+}$ and the lithology consist of heavily weathered basalts and calcrete overlying the sandstone aquifer. Since calcrete is known to be calcium rich, the high calcium content in these samples could be related to that and the basaltic plateau. High pH values ~ 8.0 - 8.5 are observed, which

favours production of bicarbonate. These water types are presented in a piper plot (Figure 4.1).

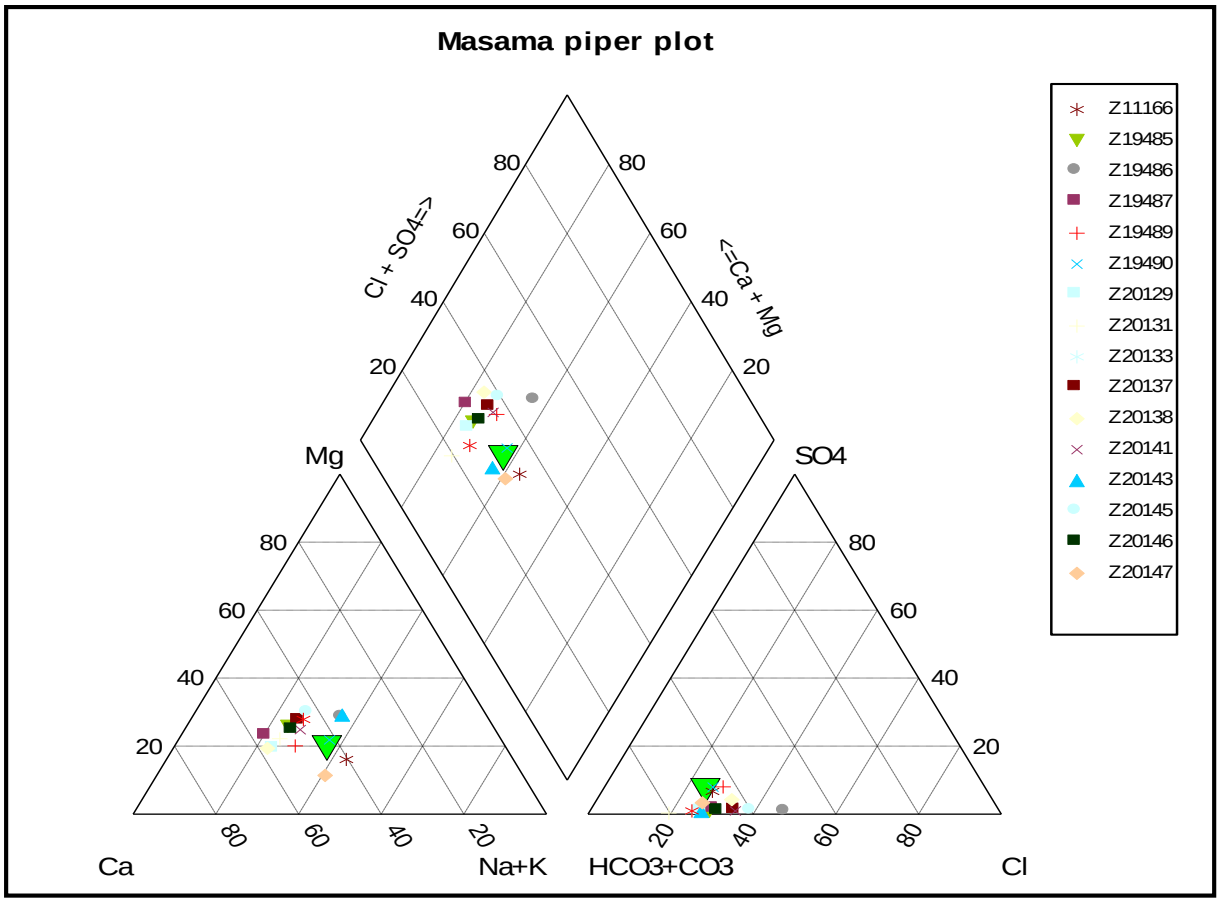


Figure 4.1 Piper plot of the Masama groundwater samples

## 4.2 Groundwater Isotopes

### 4.2.1 Stable Isotopes

The isotopic analyses results are given in Table 4.1. The groundwater samples fall below and above the local meteoric water line. The local meteoric water line used in the interpretation of the isotopic results is the Letlhakeng-Botlhapatlou Meteoric Water Line (LBMWL) which was adopted from a paper by Beekman and Selaolo (1997), $\delta^2H = 6.1*\delta^{18}O + 6.9$ ‰. The isotopic composition of groundwater in Letlakeng-Botlhatlatlou area has values of $\delta^{18}O$= -

5.54±0.22‰ and $\delta^2H$= -34.4±2.7‰ (Beekman, et al., 1997). The same spatial variation is seen in Masama with $\delta^{18}O$=-6.1±0.02‰ and $\delta^2H$=-33.7±0.07‰.

A plot of $\delta^{18}O$ and $\delta^2H$, Figure 4.2, shows two clusters of which are either depleted or enriched with respect to the rain sample collected in winter, an evaporative enrichment is observed in those samples that lie below the local meteoric line. Major difference is observed in the $\delta^2H$ values and a high d-excess is seen in the samples that lie above the LBMWL, which might be attributed to different moisture sources for the two clusters. The moisture source for depleted groundwater samples (those that lie above the LBMWL) originated from the cold air masses of the Atlantic oceans or recharged by isotopically depleted rainfall from higher altitude or heavy storms whereby aquifer replenishment is attained along preferential flow paths. The depletion also indicates that direct infiltration occurred and if evaporation had an effect, it was minimal.

On the other hand the enriched groundwater samples might have been recharged during warmer temperatures and by local rainfall or might be old groundwater within a local system whereby the same water is being recycled over and over again at low altitudes. Amount effect might also be a reason for the dissimilarities in the two groups especially on the observed variation in $\delta^{18}O$, which is mostly controlled by the degree of rain-out from the original air mass whereas differences in air mass trajectories and source of vapour will affect the isotopic composition of rain water to a lesser extent. Large rainfall events tend to produce more isotopically depleted rain waters than relatively small events. There appears to be no current mixing between the two clusters.

Table 4.1 Hydrochemical and stable isotope data for Masama groundwater

| Borehole ID | pH | EC | HCO3 | Cl | SO4 | NO3 | F | Na | Ca | K | Mg | TDS | Charge Balance | $\delta^{18}O$ | $\delta^{2}H$ | d-excess | Water Type |
|---|---|---|---|---|---|---|---|---|---|---|---|---|---|---|---|---|---|
| | | µS/cm | mg/l | mg/l | mg/l | mg/l | mg/l | mg/l | mg/l | mg/l | mg/l | mg/l | % | (‰) | (‰) | | |
| Z19485 | 8.3 | 460.0 | 170.8 | 53.7 | 3.1 | 14.0 | 0.0 | 26.6 | 47.4 | 6.9 | 17.3 | 300.0 | 5.3 | -5.4 | -34.0 | 9.0 | Ca-Mg-HCO3 |
| Z19486 | 8.1 | 833.0 | 242.8 | 127.0 | 3.7 | 17.2 | 0.1 | 64.9 | 60.7 | 9.7 | 29.9 | 540.0 | 3.8 | -7.7 | -36.5 | 25.5 | Ca-Na-HCO3 |
| Z19487 | 8.5 | 307.0 | 114.7 | 23.9 | 4.8 | 5.2 | 0.1 | 38.9 | 42.3 | 2.7 | 6.3 | 196.0 | 23.0 | -3.9 | -27.3 | 4.3 | Ca-Na-HCO3 |
| Z19489 | 8.2 | 437.0 | 167.1 | 43.0 | 17.5 | 3.2 | 0.2 | 38.5 | 62.3 | 2.7 | 15.2 | 280.0 | 16.4 | -4.5 | -28.4 | 7.8 | Ca-Na-HCO3 |
| Z19490 | 8.4 | 460.0 | 181.8 | 39.1 | 2.3 | 34.4 | 0.1 | 36.4 | 81.1 | 5.2 | 17.0 | 300.0 | 20.8 | -5.3 | -34.3 | 8.1 | Ca-Na-HCO3 |
| Z20129 | 8.2 | 445.0 | 180.6 | 44.4 | 3.8 | 14.4 | 0.0 | 26.5 | 67.8 | 2.3 | 17.0 | 280.0 | 13.9 | -5.1 | -32.0 | 8.9 | Ca-Mg-HCO3 |
| Z20131 | 8.3 | 531.0 | 237.9 | 32.3 | 1.7 | 40.3 | 0.2 | 39.2 | 84.1 | 6.1 | 21.5 | 340.0 | 17.4 | -5.2 | -33.3 | 8.6 | Ca-Na-HCO3 |
| Z20133 | 8.5 | 479.0 | 197.6 | 42.0 | 2.6 | 27.8 | 0.1 | 34.4 | 32.3 | 5.1 | 16.5 | 300.0 | -3.6 | -8.2 | -38.8 | 27.0 | Ca-Na-HCO3 |
| Z20137 | 8.0 | 482.0 | 172.0 | 54.0 | 2.8 | 29.6 | 0.0 | 28.0 | 49.8 | 8.5 | 16.1 | 300.0 | 3.6 | -7.4 | -34.8 | 24.2 | Ca-Mg-HCO3 |
| Z20138 | 8.3 | 572.0 | 234.2 | 61.1 | 3.3 | 19.6 | 0.1 | 31.0 | 58.3 | 7.0 | 18.0 | 360.0 | -0.3 | -5.4 | -33.0 | 10.3 | Ca-Mg-HCO3 |
| Z20141 | 8.0 | 428.0 | 147.6 | 54.9 | 2.6 | 15.7 | 0.0 | 25.6 | 39.0 | 4.3 | 16.6 | 280.0 | 2.9 | -7.6 | -36.8 | 24.4 | Ca-Mg-HCO3 |
| Z20143 | 8.8 | 618.0 | 289.1 | 54.3 | 4.1 | 12.9 | 0.1 | 42.2 | 71.1 | 10.1 | 27.0 | 400.0 | 8.9 | -4.5 | -31.2 | 5.0 | Ca-Mg-HCO3 |
| Z20145 | 8.6 | 572.0 | 241.6 | 56.6 | 3.4 | 18.6 | 0.1 | 34.1 | 70.1 | 7.6 | 22.4 | 360.0 | 8.4 | -8.4 | -38.7 | 28.7 | Ca-Mg-HCO3 |
| Z20146 | 8.5 | 365.0 | 150.1 | 31.1 | 12.6 | 6.2 | 0.3 | 37.6 | 40.6 | 2.4 | 11.2 | 240.0 | 11.1 | -7.7 | -35.7 | 25.8 | Ca-Na-HCO3 |
| Z20147 | 8.5 | 407.0 | 162.3 | 36.7 | 16.2 | 3.6 | 0.3 | 37.8 | 39.7 | 2.4 | 12.8 | 260.0 | 7.2 | -8.1 | -37.9 | 26.6 | Ca-Na-HCO3 |
| BH11160 | 8.1 | 337.0 | 123.2 | 28.1 | 10.3 | 19.9 | 0.1 | 33.8 | 29.3 | 2.9 | 7.2 | 220.0 | 3.5 | -4.6 | -29.9 | 7.2 | Na-Ca-HCO3 |
| BH11166 | 8.1 | 572.0 | 205.0 | 60.4 | 11.9 | 15.4 | 0.0 | 29.7 | 72.2 | 3.4 | 14.9 | 360.0 | 5.5 | -5.1 | -30.8 | 10.1 | Ca-Na-HCO3 |
| BH11168 | 8.3 | 465.0 | 195.0 | 37.5 | 0.1 | 21.7 | 0.1 | 50.0 | 41.6 | 4.0 | 8.8 | 308.0 | 4.9 | -7.7 | -35.7 | 25.5 | Na-Ca-HCO3 |

Charge balances in red greater than 10% are taken as lab errors

In case of relatively small rain events, the enrichment observed in $\delta^{18}O$ may be attributed to evaporative enrichment of raindrops below the cloud base especially in Botswana due to its climate being semi-arid while condensation may account for the $\delta^{18}O$ depletion observed in the groundwater samples (Beekman et al., 1997).

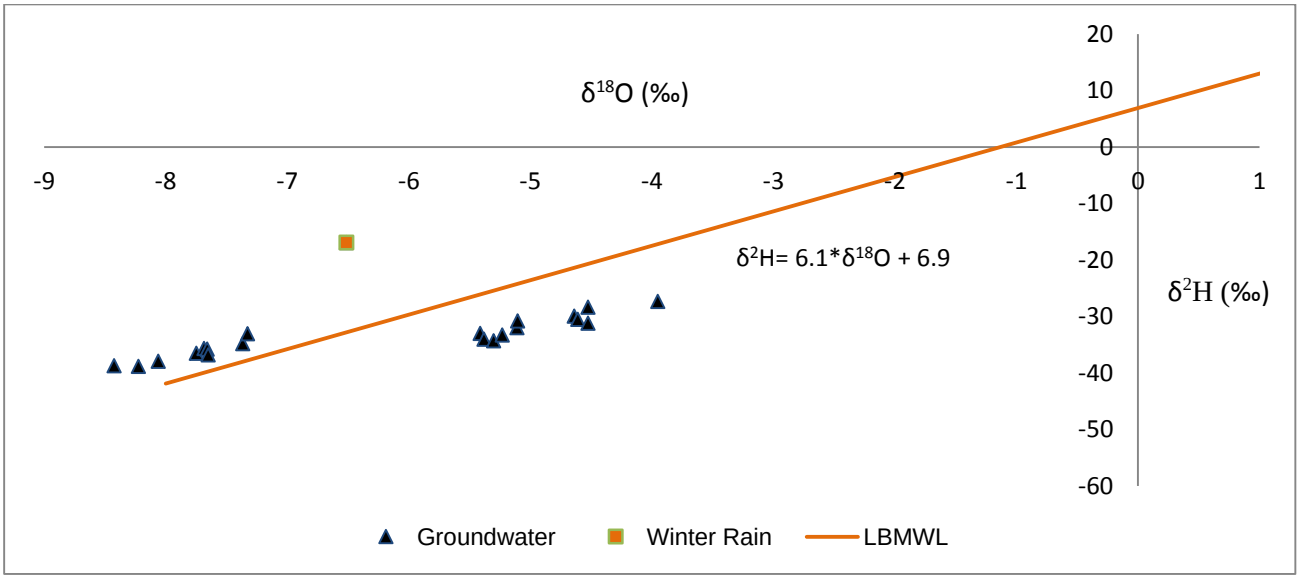


Figure 4.2 Plot of $\delta^{18}O$ and $\delta^{2}H$ for groundwater sample

The $\delta^{18}O$ values progressively decrease from northwest to southeast, which is evident in Figure 4.3. Discontinuity is observed in samples on the southern side of the Makhujwane fault where the values drop and basalts are thicker than on the northern side. The presence of "old "northwest-southeast trending horst and graben structures, of the prominent Khurutse fault might be acclaimed to this discontinuity. The boreholes situated here are encompassed by three faults, which are the Khurutse, Makhujwane and Seswana Faults.

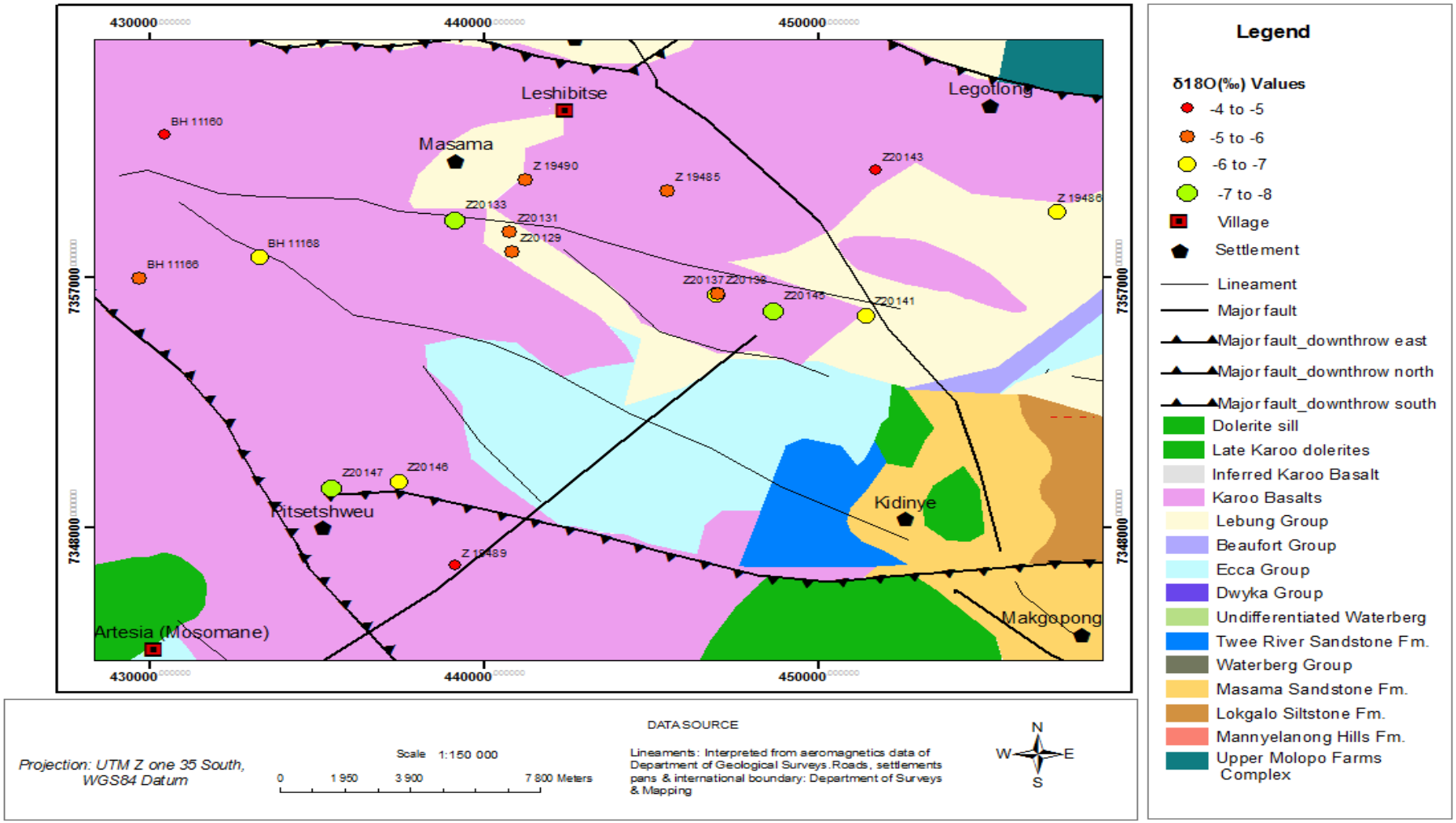


Figure 4.3 Distribution of $\delta^{18}O$ in study area

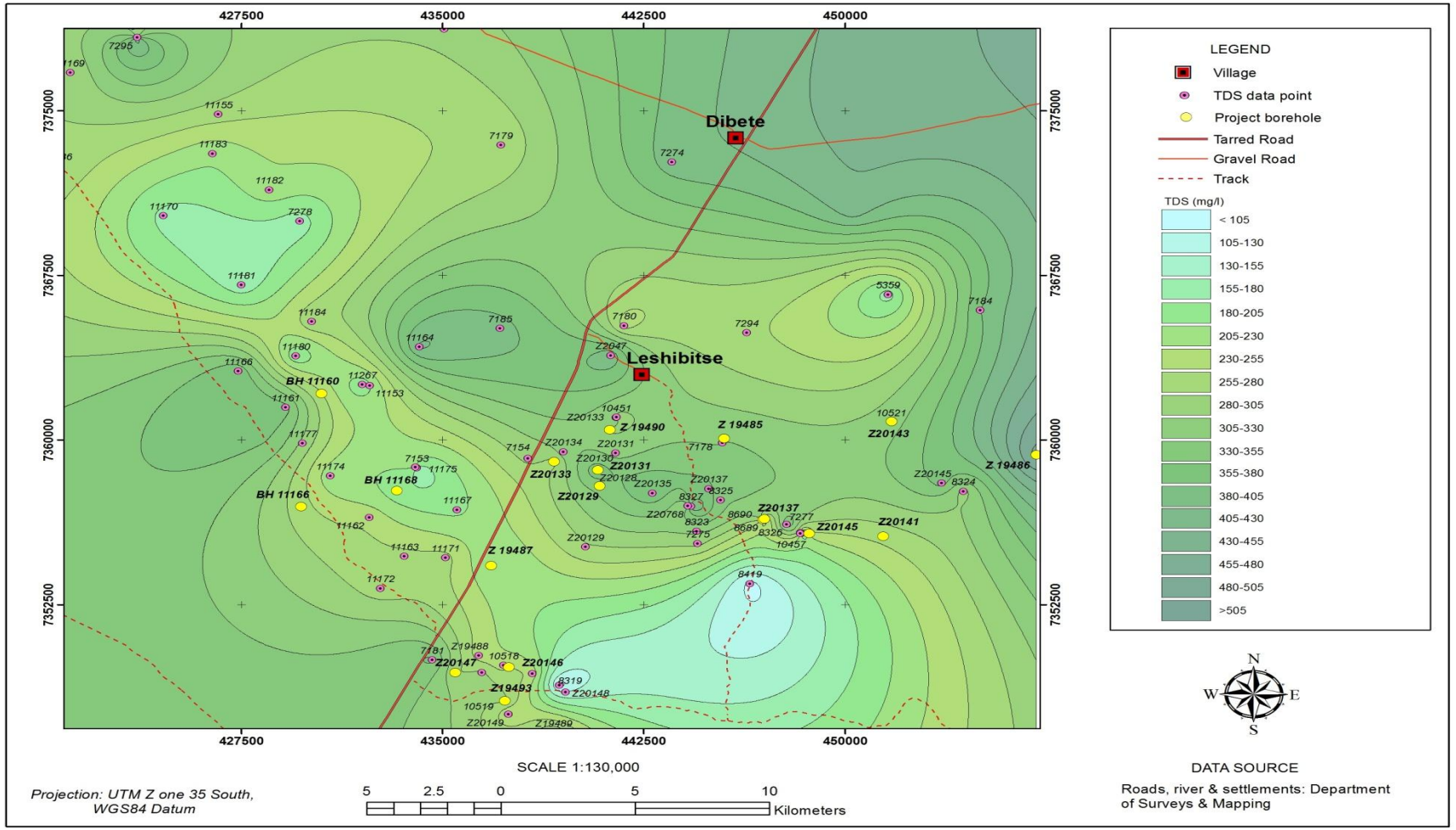


Figure 4.4 TDS distribution in study area

### 4.2.2 Radioactive Isotopes

The groundwater in the Masama aquifer can be characterised most easily by categorising them two general groups:

1) modern, or recharge water, which contains detectable amounts of tritium and in general is associated with water draining from the Dibete areas and those in unconfined areas on the eastern side of the study area and:

2) submodern water, which contain little or no tritium, and which occur on the western extremes, where the overlying basalt rocks are thicker.

In order to properly discuss the characteristics of these two groups, location and extent of the recharge areas must first be discussed, as well the possible influences by the structures present in the area on modern recharge.

Authors such as Fontes and Garnier (1979), Han et al. (2012), Plummer and Glynn (2013) justified in their works that the initial $^{14}C$ concentration in pre-bomb groundwater can vary depending on the host rock in the aquifer and on whether the reactions occur in the aerated or saturated zone. In carbonate and silicate rocks the initial $^{14}C$ can vary between 50-100 pmc respectively. Eichinger (1983) comments that in reality a drop of 65 % initial $^{14}C$ in carbonate rocks is linked to water-rock interaction during periods of recharge while a drop of 90 % is attributed to silicate rocks (volcanics, quartzites and sandstones). These values can be used to calculate the age of older groundwaters only if the local groundwater is abstracted within the same type of rocks. During recharge the $CO_2$ (100 pmc) and carbonates rock (0 pmc) react to form dissolved bicarbonate (50 pmc). In silicates the initial $^{14}C$ concentration is usually closely preserved (Eichinger, 1983).

#### 4.2.2.1 Extent of Recharge Areas and Possible Structural Influence on Groundwater Chemistry

The presence of Tritium in groundwater substantiates that active recharge takes place, but due to mixing of groundwater in the aquifer, refined groundwater age interpretations have long been a challenge and for that Tritium as a standalone tracer is only used to provide qualitative circulation time. Plots of Tritium against $\delta^{18}O$ could be used to get an insight into the recharge or circulation zones of the ground; refer to Figure 4.6. In this plot two distinct groundwater flow systems are represented with some boreholes pumping deep circulating waters whilst others abstract shallow circulating groundwater. Most of the boreholes that fall in the deep circulation zone are those drilled to the west of the study area where the basalt is very thick and can go as deep as 350 m. Groundwater in this zone is characterised by high $^{18}O$ values and low $^{3}H$ values compared to the summer rain values (-6.5 ‰ and 0.2 TU). This indicates that the recharge occurred more than 50 years ago during summer but the recharge water was exposed to evaporation prior to infiltration, hence the enrichment in the $^{18}O$ values.

Table 4.2 contains results of the Tritium and radiocarbon analyses where tritium values for 15 out of 19 sampled borehole fall between 0.1- 1.5 TU indicating that the waters were recharged prior to 1952 and were in circulation for long time. Therefore, 14C values were used to estimate the circulation time of water, where the values range from 96.5 pmc to 1.4 pmc with the age range of 300 to 35,300 years.

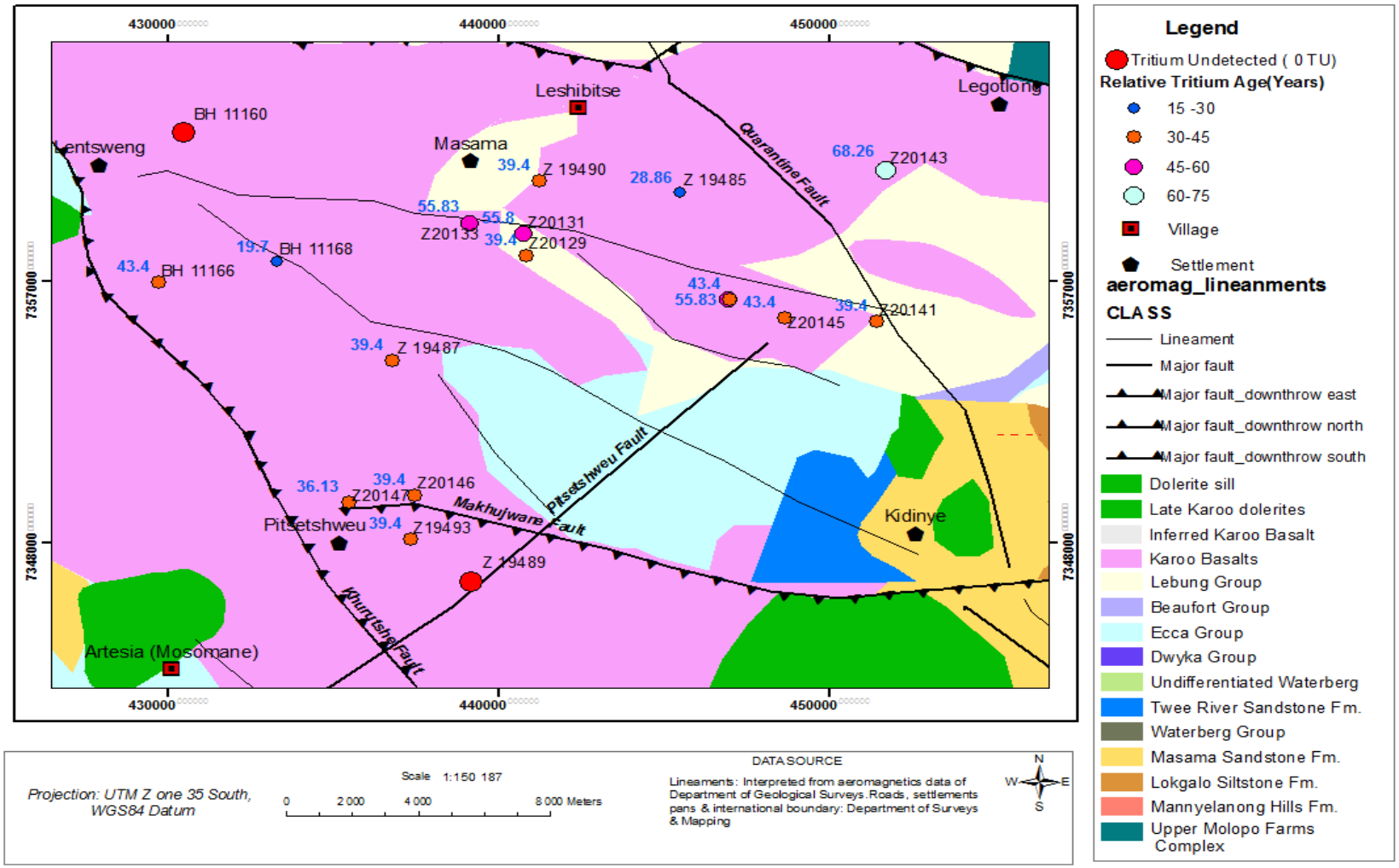


Figure 4.5 Relative tritium ages for Masama Sandstone groundwaters

Table 4.2 Calculated tritium and uncorrected Carbon-14 relative ages of the groundwaters

| Borehole Number | Tritium (T.U) | | Carbon-14 (pmc) | | Uncorrected Carbon-14 Age Years | |
|---|---|---|---|---|---|---|
| Z19485 | 0.9 | ±0.3 | 88.5 | ±2.4 | 1000 | ±10 |
| Z19486 | 0.5 | ±0.2 | 96.5 | ±2.5 | 300 | ±5 |
| Z19487 | 0.5 | ±0.2 | 47.7 | ±2.1 | 6100 | ±10 |
| Z19489 | 0.0 | ±0.2 | 15.7 | ±1.7 | 15300 | ±10 |
| Z19490 | 0.5 | ±0.2 | 64.9 | ±2.2 | 3550 | ±10 |
| Z19493 | 0.5 | ±0.2 | | | | |
| Z20129 | 0.5 | ±0.2 | 81.2 | ±2.4 | 1700 | ±10 |
| Z20131 | 0.2 | ±0.2 | 56.5 | ±2.1 | 4700 | ±10 |
| Z20133 | 0.2 | ±0.2 | 64.0 | ±2.2 | 3700 | ±10 |
| Z20137 | 0.2 | ±0.2 | 56.3 | ±2.1 | 4750 | ±10 |
| Z20138 | 0.4 | ±0.2 | 54.8 | ±2.1 | | |
| Z20141 | 0.5 | ±0.2 | 64.9 | ±2.2 | | |
| Z20143 | 0.1 | ±0.2 | | | | |
| Z20145 | 0.4 | ±0.2 | | | | |
| Z20146 | 0.5 | ±0.2 | 4.9 | ±1.5 | 24950 | ±10 |
| Z20147 | 0.6 | ±0.3 | 1.4 | ±1.5 | 35300 | ±10 |
| BH11160 | 0.0 | ±0.2 | 18.0 | ±1.7 | 14200 | ±10 |
| BH11166 | 0.4 | ±0.2 | 47.2 | ±2.1 | 6200 | ±10 |
| BH11168 | 1.5 | ±0.3 | 58.1 | ±2.2 | 4500 | ±10 |
| Rainwater | 0.2 | ±0.2 | | | | |

Contrary to this finding the TDS and chloride content in these boreholes are very low, ranging 196 -540 mg/l and 28 -127 mg/l, respectively (Figure 4.4 and Figure 4.7). An explanation for the low TDS values might be that some recent water could be reaching down through faults or fractures in the bedrock or low water-rock interaction. Using position of these boreholes and the distribution of the Tritium content relative to the major fault (Khurutse and Makhujwane) it can be conclude that this fault might be semi permeable and thus act as a route for the recharge.

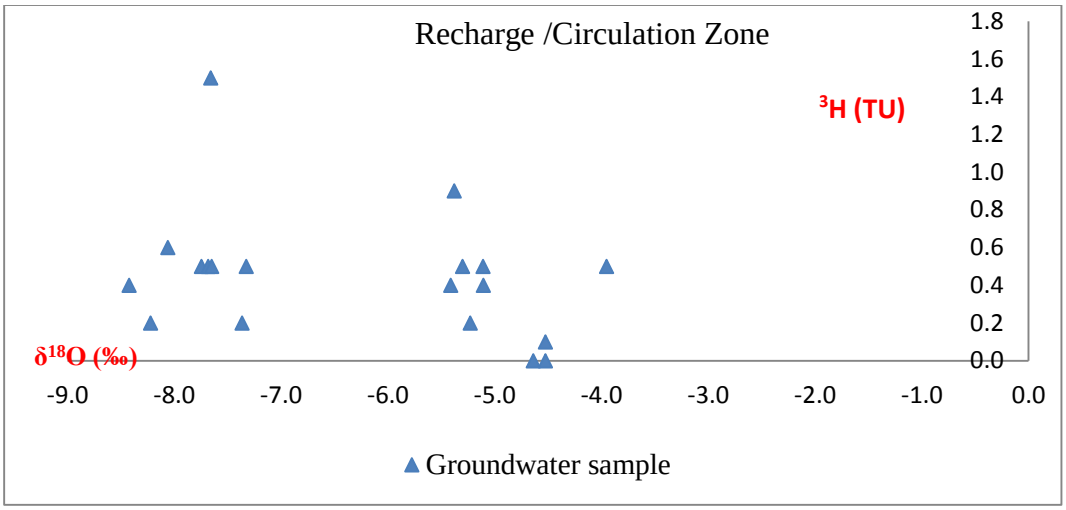


Figure 4.6 Tritium distribution with respect to $\delta^{18}O$ showing provenance of circulation

The low chloride content across the MSA, which does not seem to change much with respect to depth to the top of the aquifer i.e. thickness of basalt cover, could signify high groundwater recharge as chloride content depends on the size of the sediment pores, the initial content in the infiltrated water and evaporation. The chloride concentration in this area is controlled by the main aquifer lithology (sandstone) and the initial concentration in the recharge water which is supported by the low mineralisation and TDS values. High chloride content at Z19486 (Figure 4.7) could also be linked to low groundwater recharge during colder climate which is observed in the depleted $\delta^{18}O$ content (-7.7 ‰).

Recharge values were calculated using the Chloride Mass Balance ( CMB) method and values obtained seem to agree with the above concept with the highest chloride content (127 mg/l) corresponding to the lowest recharge rate of 4 mm/annum whilst the recharge rate for the lowest chloride content at Z19485 is 10 mm/annum therefore indicating higher recharge rate. Corresponding transmissivity and hydraulic conductivity are 50 $m^{2}$/day and 0.38 m/day for the low recharge area and 155 $m^{2}$/day and 1.55 m/day for the high recharge area. Table 4.3 contains

the calculated recharge rate following the equation from Selaolo (1998) and the total annual chloride deposition rate ( $T_D$) values range between 400 – 750 mg/m$^2$/annum.

$$\mathbf{R = P * Cl}_{wad} \mathbf{/ Cl}_{gw} = T_D / Cl_{gw}$$

Where **P** = Mean Annual Precipitation (mm/annum)

**Cl** $_{wad}$ = Total Chloride Deposition (Wet & Dry Deposition) (mg/l)

**Cl**$_{gw}$ = Chloride Concentration in groundwater (mg/l)

$T_D$ = **P * Cl** $_{wad}$ **=** Total Annual Chloride Deposition Rate (mg/m2/annum)

Table 4.3 Recharge rates calculated using Chloride Mass Balance method

| **Borehole Id** | **Date Sampled** | **Cl in Groundwater** | **Recharge (mm/annum) at various Cl deposition rate ($T_D$ - mg/m2/annum)** | | | **Average Recharge** |
|---|---|---|---|---|---|---|
| | | **mg/l** | **$T_D$ - 400** | **$T_D$ - 525** | **$T_D$ - 750** | **(mm/annum)** |
| Z19485 | 21/06/2016 | 53.7 | 7 | 10 | 14 | 10 |
| Z19486 | 22/06/2016 | 127.0 | 3 | 4 | 6 | 4 |
| Z19487 | 27/06/2016 | 23.9 | 17 | 22 | 31 | 23 |
| Z19489 | 27/06/2016 | 43.0 | 9 | 12 | 17 | 13 |
| Z19490 | 26/06/2016 | 39.1 | 10 | 13 | 19 | 14 |
| Z20129 | 27/06/2016 | 44.4 | 9 | 12 | 17 | 13 |
| Z20131 | 22/06/2016 | 32.3 | 12 | 16 | 23 | 17 |
| Z20133 | 22/06/2016 | 42.0 | 10 | 13 | 18 | 13 |
| Z20137 | 22/06/2016 | 54.0 | 7 | 10 | 14 | 10 |
| Z20138 | 26/06/2016 | 61.1 | 7 | 9 | 12 | 9 |
| Z20141 | 22/06/2016 | 54.9 | 7 | 10 | 14 | 10 |
| Z20143 | 23/06/2016 | 54.3 | 7 | 10 | 14 | 10 |
| Z20145 | 23/06/2016 | 56.6 | 7 | 9 | 13 | 10 |
| Z20146 | 27/06/2016 | 31.1 | 13 | 17 | 24 | 18 |
| Z20147 | 27/06/2016 | 36.7 | 11 | 14 | 20 | 15 |
| BH11160 | 28/06/2016 | 28.1 | 14 | 19 | 27 | 20 |
| BH11166 | 27/06/2016 | 60.4 | 7 | 9 | 12 | 9 |
| BH11168 | 26/06/2016 | 37.5 | 11 | 14 | 20 | 15 |

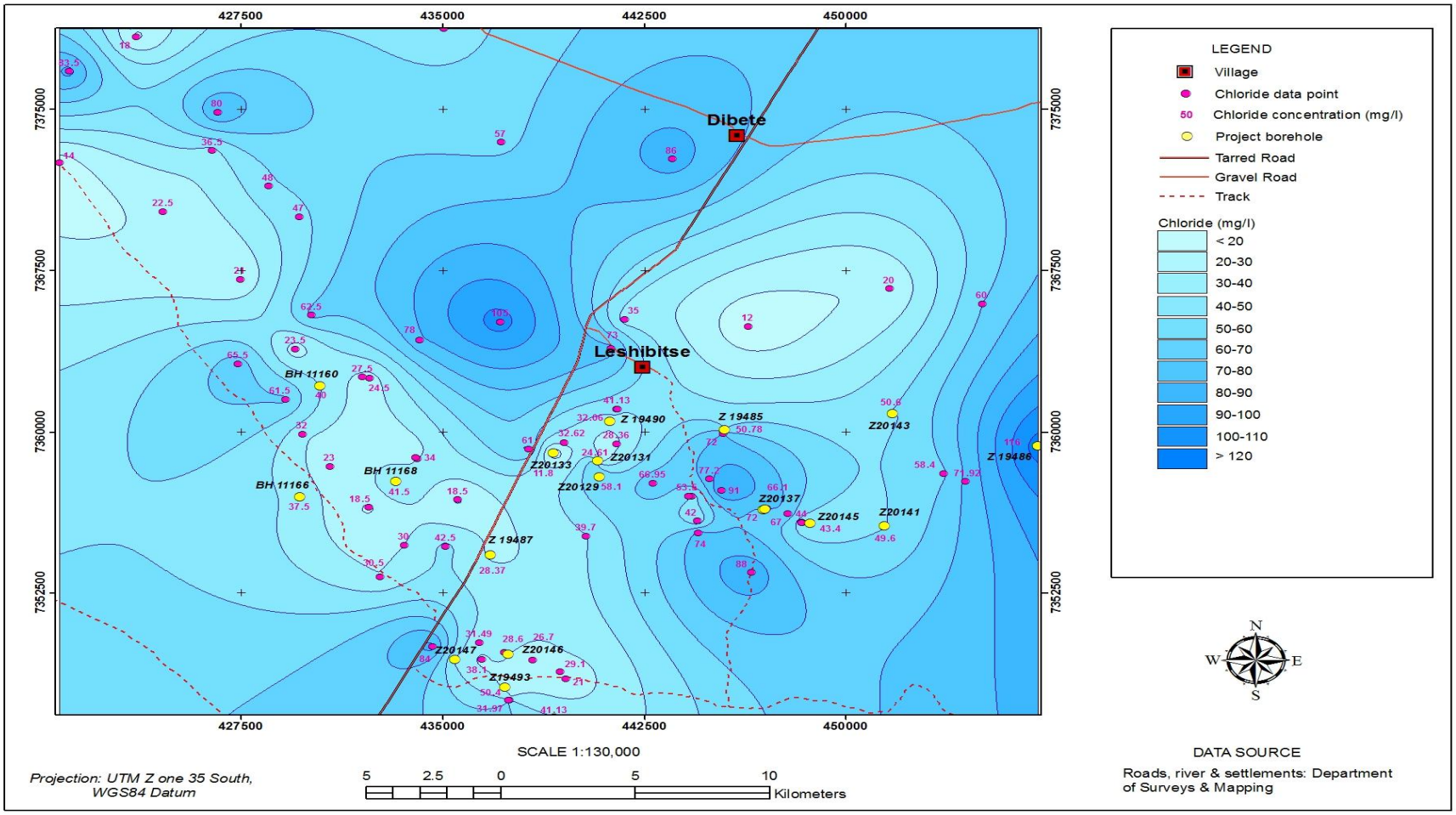


Figure 4.7 Chloride distribution in study area

The use of $^{14}C$ further supports the two above mentioned areas (Z19485 and Z19486) as recharge zone, with values of 88.5 pmc and 96.5 pmc. Since pre-1952 $^{14}C$ was about 100 pmc, the waters have either retained almost all of their initial carbon-14 or indeed recharged does occur in the areas.

Verhagen et al. (1974) and Leaney and Allison (1986) comment that any concentration of water that was recharged preferably before pre-1952's when the atmospheric $^{14}C$ was 100 pmc should not be affected. This hypothesis though, is only valid if a closed system is assumed, that is there is no $^{14}C$ exchange with the atmosphere. High concentrations of $HCO_3^-$, approximately 100 -300 mg/l also supports this hypothesis as it seems from these concentrations there was lose of $^{14}C$ due to reactions with rocks and addition of "dead " carbon by interaction with aquifer rocks.

This fact reflects that even though the groundwater in this area was recharged prior to 1952 the changes seen in the $^{14}C$ results are controlled more by geochemical reactions in the aquifer. Reverse cation exchange is observed on the western side of the study area where more sodium is detected in groundwater samples. Carbonate reaction in the centre and eastern part of the area, especially where the basalt is thin or absents accounts for the high calcium. Values of 14C near 100 pmc, could also mean that the recharge rate is low or it is restricted to certain areas of the aquifer and not all the faults act as route for recharge. The northern part (where Z19485 is situated) was hypothesised to act as the recharge area feeding the downflow lower half of the aquifer, this decision was influenced by the flow direction from the piezometric surface map and the observation made is that, carbon-14 ages decrease along flow in a NW-SE direction (Figure 4.8) whilst tritium ages increase. For both isotopes, a break in age is encountered once the area changes between unconfined and confined conditions, becoming either older or younger. This shows that when it comes to age and recharge, the overlying strata and lineaments do play a role.

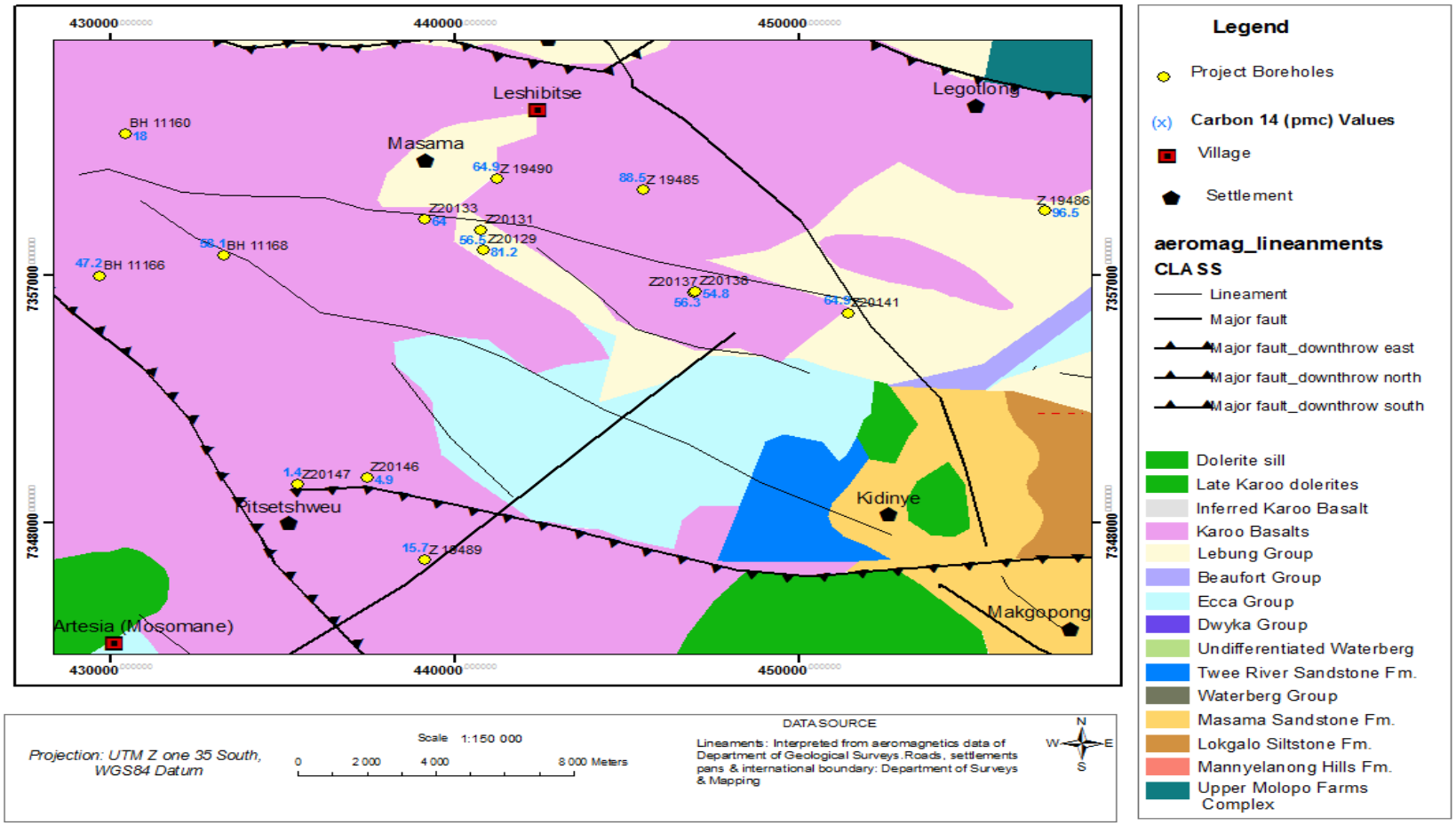


Figure 4.8 Distribution of 14C in study area

## 4.3 Application of Multivariate Statistics to Masama Ntane Sandstone Aquifer

### 4.3.1 Hierarchical Component Analysis

Hierarchical Component analysis sorts the observed data into their meaningful clusters in a hierarchal order restricting each cluster to a specific water quality property and location. Even though the piper plot diagram has only one cluster, it was essential to identify the similarity among the samples and hence HCA was applied. Two clusters were determined from the 9 variables that were chosen. These variables were pH, $Na^+$, $K^+$, $Ca^{2+}$, $Mg^{2+}$, $Cl^-$, $HCO^-_3$ and $SO_4^{2-}$ excluding variables such as total dissolved solids, alkalinity and electrical conductivity which are dependent on each other to reduce redundancy. The outcome of the iteration is a dendrogram (Figure 4.9) which lists the clusters in an increasing order of $Na^+$, $K^+$, $Cl^-$, and $SO_4^{2-}$ from right to left.

In cluster I, 12 boreholes are grouped under this cluster. These boreholes are located in the part of the study area were the basalt thickness varies, ranging around 60-250 m deep and characterised by TDS below 400 mg/l of which signifies low water-rock interactions. Major fault zone were targeted for placement of these boreholes. Those boreholes situated where the basalt is thin or the Kalahari beds are thicker show a slight enrichment in the heavy isotope which might be inferred to evaporation. The $\delta^{18}O$ enrichment ranges between -5.1 to -3.9 ‰ compared to the summer rain, $\delta^{18}O$ = -6.5 ‰. The tritium values are between 0.0 - 0.6 TU which indicates that the water is old, probably recharged around 10-50 years ago, by different sources within a local flow system or when temperatures were warmer. The other boreholes four boreholes (Z20146,

Z20147, Z20145 and Z20133) with depleted $\delta^{18}O$ value of -7.7 to 8.4 ‰ could be part of a regional flow system where recharge occurs in preferential flows by diffuse sources.

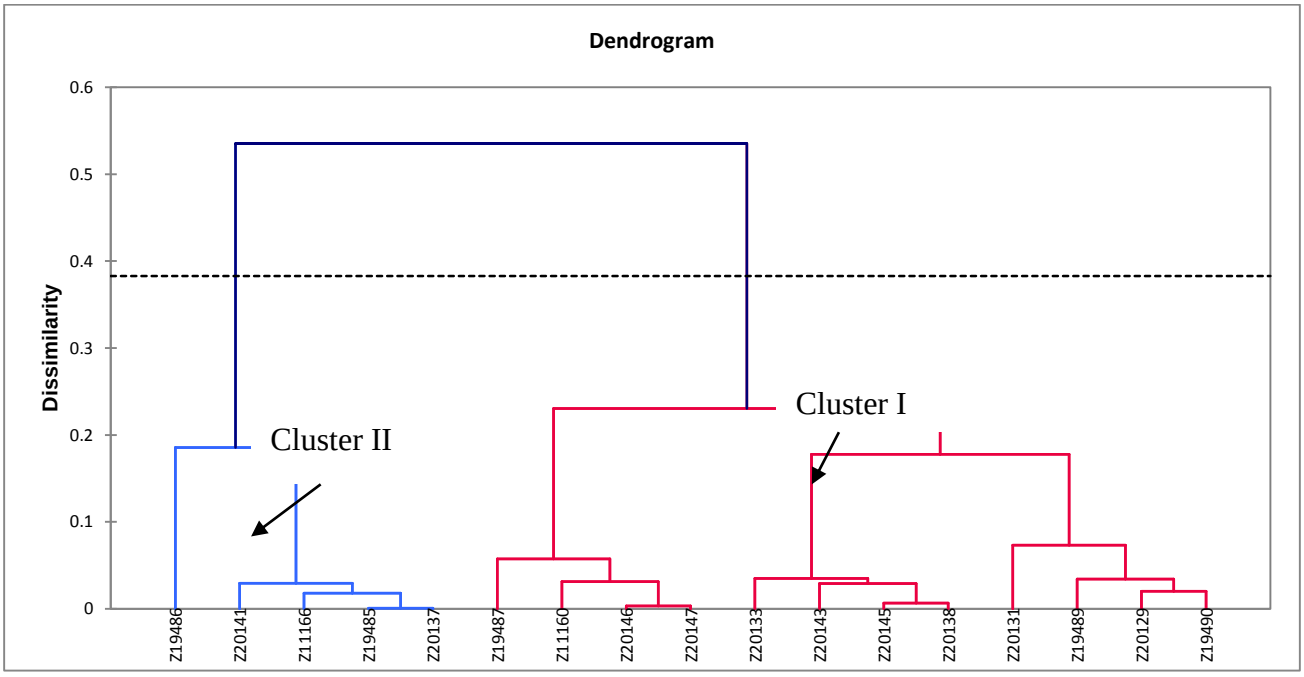


Figure 4.9 Dendrogram of groundwater samples

Cluster II consists of 5 boreholes (Z20137, Z19486, Z19485, BH11166 and Z20141) which are located in the transition zone between the thin and the thicker basalts areas. Similar geology as in Cluster I is intercepted but the basalt is either thin approximately 20-50 m with most part of it being heavily weathered, rendering it almost absent in some boreholes. The dominant ions in this group are $Ca^{2+}$, $Mg^{2+}$ and $HCO_3^-$ same as in cluster I. However, the $Na^+$ and $SO_4^{2-}$ concentrations in this cluster are lower compared to cluster I, whilst the $K^+$, $Ca^{2+}$, $Mg^{2+}$, $Cl^-$, $HCO_3^-$ concentrations are increased. These boreholes have higher salinity compared to cluster I, with TDS range of 300 - 540 mg/l. Although in the same cluster, borehole Z19486, which is unconfined, has the highest TDS value, 540 mg/l relative to all sampled boreholes. The hydraulic gradient in this area is nearly flat, producing slow groundwater velocity. This leads to the long

residence time of the waters in the host rocks, hence enhancing a strong water-rock interaction. $Na^+$, $Ca^{2+}$, $Cl^-$, $HCO_3^-$ are the major constituents. The chloride and magnesium concentration is considerably high with a value of 127 mg/l and 29.9 mg/l comparative to other boreholes in both the two clusters, which range 53-60 mg/l and 6 - 27 mg/l respectively. The high chloride content could be reason for the elevated TDS value whilst the high $Mg^{2+}$ level could be linked to its precipitation as Mg-silicates when Na-silicates mineral dissolve along groundwater flow direction.

Z19486 is also depleted in heavy isotopes (-7.7 ‰ $\delta^{18}O$ and -36.5 ‰ $\delta^{2}H$) with respect to the winter rain sample collected. The reason might be that recharge occurred under cold air conditions and direct infiltration. However, the shift in oxygen could indicate high residence time and deep circulation which allowed fractionation. Geochemical reactions that involve alteration of silicate mineral such as plagioclase can also cause a shift in $\delta^{18}O$.

$Na\text{-}Ca\text{-}HCO_3$ ($Ca\text{-}Na\text{-}HCO_3$) water + plagioclase (Na-Silicate minerals) $\rightarrow$ $Na\text{-}HCO_3$ water + clay precipitated Ca (Mg)-silicates)

The average isotopic composition in clusters I and II is -33.7 ‰ $\delta^{2}H$ and -6.1 ‰ $\delta\ ^{18}O$, of which the oxygen content value is nearer to the average summer rainfall. In the contrary, the deuterium value is almost twice the value of rainfall, which might owe to heavy rain event that falls on highlands under cold air conditions and probably some silicate weathering as the aquifer is composed of sandstone. Fractures, faults and high hydraulic gradients associated with the area especially at highlands may influence the hydrological processes in these clusters. A general representation of the hydrochemical reaction in these clusters can be represented as:

Silicic rock + Rainwater →Na –Ca-$HCO_3$ (Ca-Na-$HCO_3$) water + altered rock

### 4.3.2 Statistical Correlation and Principal Component Analysis

To better understand the interrelationship between physiochemical variable of the sampled boreholes, statistical correlation and principal component analysis has been used as the assessment tool. Principal component is a mathematical technique that reduces dimensionality by creating a new set of variables called principal components. These are created to maximise the amount of variance whilst remaining uncorrelated with the other components (Belkhiri, 2011). The expected outcome of this method is to understand the hydrochemical evolution processes and the underlying geochemical reaction within the Masama aquifer. The principal component loading has the effect of producing results on the bases of loading factors in which some factors will have high loading or near-zero loading on others ( Wang et al., 2001). This concept makes interpretation of variables easier as it maximises the differences and make it more easier to pick the variable that are more influential.

Correlation describes the strength of a relationship between two variables. Correlation coefficients range between -1 to +1. Correlation value of +1 indicates a perfect positive linear relationship between variables while -1 indicates a perfect negative linear relationship. On the other hand a value of 0 indicates that there is no linear relationship, the variables are uncorrelated. The correlation coefficients normally lies somewhere between these values. In groundwater studies, negative correlation is linked to occurrence of competitive processes (Ghesquière, 2015).

The statistical correlation results are shown in Table 4.4 and from it, $Na^{+}$, $k^{+}$, $Ca^{2+}$, $Mg^{+2}$, $Cl^{-}$, $HCO_3^{-}$ and $CO_3^{-2}$ show a weak to strong positive correlation with each other. The strongest

positive correlation is seen between $K^+$, $Mg^{2+}$ and $HCO_3^-$ while $Na^+$, $Ca^{2+}$ and $CO_3^{-2}$ are weak to nearly uncorrelated. On the other hand, these are negatively correlated to pH and $SO_4^{-2}$. The source of $Na^+$ and $K^+$ could be weathering of feldspars and clays while cation exchange (exchange of $Ca^{+2}$ for $Na^+$) accounts for the increased calcium in groundwater samples along flow path as basalts are drained.

Principal component analysis was used to explain the contribution of aquifer properties and geochemical reaction processes to the observed water quality. Basic principles and application to hydrogeology can be found in numerous literatures (Helena et al. 2000; Papatheodorus et al., 2007; Moya et al., 2015; Hussin et al., 2016). The fist principal component is a linear combination of the original variables and explains much variation as possible in the original data. Each subsequent principal component explains much of the remaining variation as possible, under the condition that it is uncorrelated with the previous component (Anderson, 1984 and Davis, 2002).

Table 4.4 Correlation matrix (Pearson (n))

| Variables | pH | $Na^+$ | $K^+$ | $Ca^{2+}$ | $Mg^{2+}$ | $HCO^-_3$ | $CO^{-2}_3$ | $Cl^-$ | $SO^{-2}_4$ |
|---|---|---|---|---|---|---|---|---|---|
| pH | 1.00 | -0.34 | -0.76 | -0.36 | -0.86 | -0.70 | -0.36 | -0.62 | 0.57 |
| $Na^+$ | -0.34 | 1.00 | 0.35 | 0.16 | 0.48 | 0.36 | 0.22 | 0.57 | 0.07 |
| $K^+$ | -0.76 | 0.35 | 1.00 | 0.34 | 0.81 | 0.75 | 0.52 | 0.63 | -0.60 |
| $Ca^{2+}$ | -0.36 | 0.16 | 0.34 | 1.00 | 0.58 | 0.65 | 0.30 | 0.21 | -0.23 |
| $Mg^{2+}$ | -0.86 | 0.48 | 0.81 | 0.58 | 1.00 | 0.89 | 0.51 | 0.74 | -0.44 |
| $HCO^-_3$ | -0.69 | 0.36 | 0.75 | 0.65 | 0.89 | 1.00 | 0.69 | 0.52 | -0.36 |
| $CO^{-2}_3$ | -0.36 | 0.22 | 0.52 | 0.30 | 0.51 | 0.69 | 1.00 | 0.03 | -0.20 |
| $Cl^-$ | -0.62 | 0.57 | 0.63 | 0.21 | 0.74 | 0.52 | 0.03 | 1.00 | -0.24 |
| $SO^{-2}_4$ | 0.57 | 0.07 | -0.60 | -0.23 | -0.44 | -0.36 | -0.20 | -0.24 | 1.00 |

The variance shows the amount of variation in the original data explained by each PC. Standardisation of data is done and this ensures that a PC with variance of 1 account for variation equivalent to 1 of the original variables. Also the sum of the variables equal to the number of original variables. Absolute values near 0 indicate that a variable contributes little to the component while larger absolute values indicate that a variable contributes more. The proportion of each variable‘s variance that can be explained by the factors (e.g the underlying latent continua) is termed the communality. This basically means the sum of squared factor loadings for the variable, denoted as $h^2$ (Davis, 2000).

The correlation monoplots show vectors plotting away from the origin to represent the original variables. The first principal component accounts for 55.58 % (Table 4.5 and Figure 4.10) of the total variance and shows substantial positive loading for $K^+$, $Mg^{2+}$, $Cl^-$, and $HCO_3^-$, with a moderate positive loading for $Na^+$, $Ca^{+2}$ and $CO_3^{2-}$; a high negative loading for pH and a moderate negative loading for $SO_4^{-2}$. This PC corresponds to cluster II of the HCA classification, representing the lowlands and can be considered as the mineralisation axes.

Table 4.5 PC loadings after rotation

| | PC1 | PC2 | PC3 | Communality |
|---|---|---|---|---|
| pH | -0.866 | -0.005 | 0.276 | 0.75 |
| $Na^+$ | 0.496 | 0.684 | 0.295 | 0.93 |
| $K^+$ | 0.889 | -0.053 | -0.196 | 0.79 |
| $Ca^{2+}$ | 0.574 | -0.283 | 0.354 | 0.42 |
| $Mg^{2+}$ | 0.971 | 0.066 | 0.029 | 0.95 |
| $HCO_3^-$ | 0.908 | -0.162 | 0.273 | 0.85 |
| $CO_3^{2-}$ | 0.572 | -0.401 | 0.502 | 0.51 |
| $Cl^-$ | 0.708 | 0.577 | -0.233 | 0.95 |
| $SO_4^{-2}$ | -0.538 | 0.429 | 0.622 | 0.51 |
| Explained variance (%) | 55.581 | 13.98 | 12.173 | |
| Cumulative of variance (%) | 55.581 | 69.561 | 81.734 | |

Potassium concentrations are low, ranging 2-9 mg/l for all groundwater samples. These low concentrations could be related to the fact that generally, potassium minerals are resistant to weathering (Hem, 1985).

The second PC accounts for 13.98 % of the total variance. It has significant positive loading for $Na^+$ and $Cl^-$ and a moderate positive loading for $SO_4^{-2}$. A poorly negative loading is seen for the $Ca^{2+}$ and the opposite loading between $Ca^{+2}$ and $Na^+$ on this factor plane can be associated with cation exchange reaction between the two along the flow direction. This PC corresponds to cluster I which represents the highlands. An enrichment of $\delta^{18}O$ accompanies this geochemical reaction but an abrupt depletion is in seen once a boundary (Makhujwane fault) is encountered.

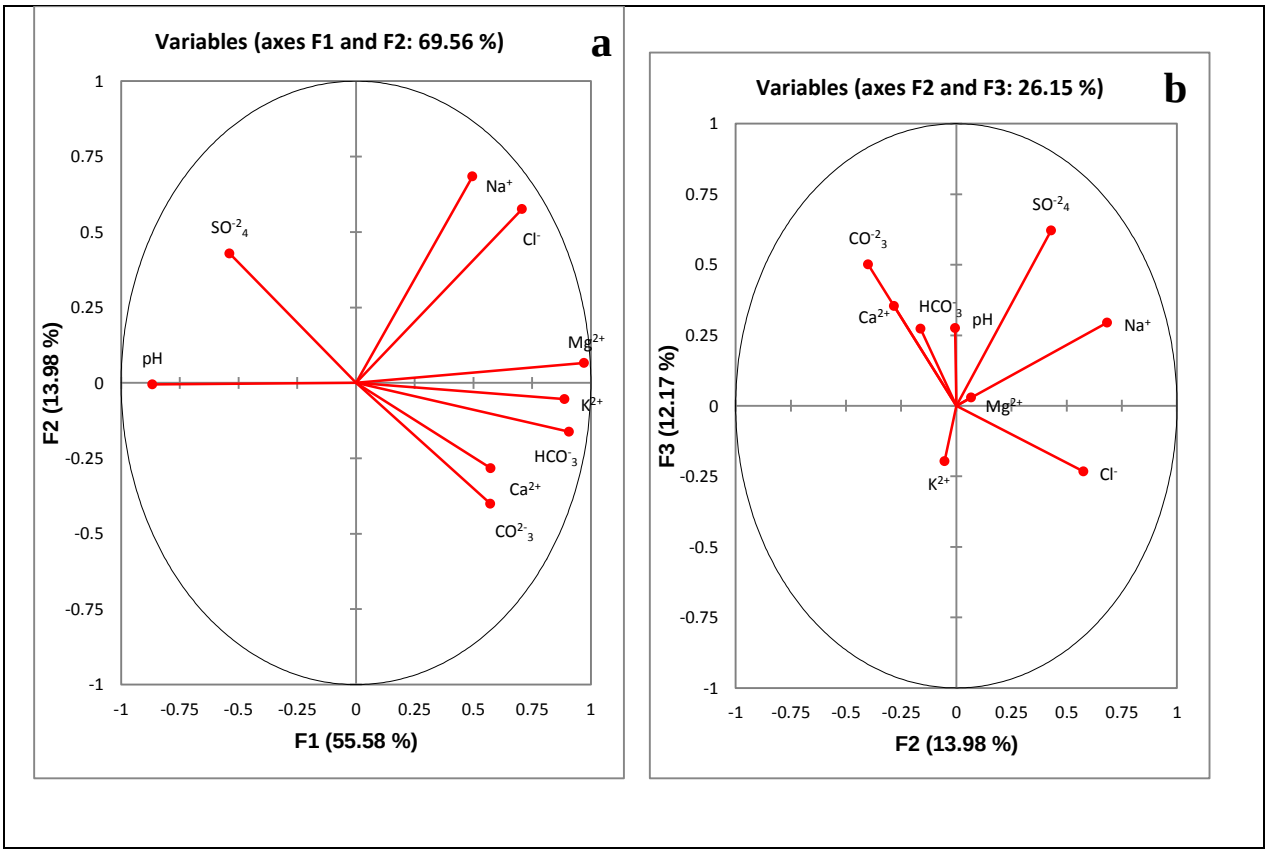


Figure 4.10 Variables projection on PC planes: PC1 and PC2 (a), PC2 and PC3 (b).

# 5 CONCLUSION AND RECOMMENDATIONS

## 5.1 Conclusion

The integrated use of isotopic and hydrogeochemical analyses was employed to investigate the Masama Sandstone Aquifer. Aspects of interest were the factors that control the groundwater composition, source of recharge and the related mechanism in this area. Groundwater is considered to be fresh water with low mineralisation as seen in TDS values ranging from 196-540 mg/l. In areas where the basalt is thick basin $Na^{+}$- $HCO_3^{-}$ water type predominate even though the pier picks only one general $Ca^{+}$- $HCO_3^{-}$ water type across the basin.

Further analysis of the data using multivariate statistics techniques showed that the groundwater in the western area extremes, moving towards the centre is classified by a transition from $Ca^{+2}$- $HCO_3^{-}$ > $Na^{+}$- $Ca^{+2}$- $HCO_3^{-}$ > $Ca^{+2}$- $Na^{+}$- $HCO_3^{-}$-water type induced by cation exchange. On the other hand, the groundwater from the middle of the basin to the eastern region is categorised by $Ca^{+2}$- $Mg^{2+}$- $HCO^{-}_3$ - type, with an increase in $Na^{+}$ towards areas where the basalt is thin and the sandstone is unconfined. The $Mg^{2+}$ is probably introduced by precipitation of Mg-silicates when Na-silicates minerals dissolve along groundwater flow direction.

Results of the stable isotope show two groups of groundwaters recharged under differing weather conditions and varying moisture sources. No samples lie on the LBLMW line signifying minimal possibility for groundwater mixing. Recharge in the study area occurred in both summer and winter with those groundwaters recharged in summer having enriched $\delta^{18}O$ values due to evaporative effects and plot below the LBLMW line whilst those recharged in winter have depleted $\delta^{18}O$ as a result of condensation and plot above the line. Origin of moisture source that

is, whether from high or low altitudes also attributed to the fractionation producing either isotopically depleted or enriched rainfalls that directly replenished the aquifer.

Based on the $\delta^{18}O$ and $^{3}H$ distribution low Tritium concentration below 0.8 TU indicates deeper circulation of groundwater and older ages. This also testifies that the recharge occurred when the climate was colder than today and lack of influence from modern day meteoric water. Groundwaters in the extremes of the basin are relatively enriched in $\delta\ ^{18}O$ compared to those towards the centre of the basin; this indicates lack of a strong subsurface link between low basaltic plateau and the highlands.

The relative enrichment can be related more to the different sources of recharge or degree of circulation than evaporative effect there as there is still a reasonable coverage in these areas. A probable cause could be direct recharge by isotopically enriched groundwaters. Groundwaters of this type are seen at Z19489 and Z11160 recording 0.0 TU showing that the water is too old for Tritium age dating. The same groundwaters have $^{14}C$ values of 15.7 pmc and 18.0 pmc respectively; showing that recharge in these locations occurred around 14700 to 15300 years ago as seen from the carbon-14 scale.

On the other hand, high Tritium values with corresponding enriched $\delta^{18}O$ values justifying a hydrologic communication between the aquifer and atmosphere and marks the shallow circulation zones. Tritium dating method identifies locations at Z11168 and Z19485, as possible recharge zones with relative age of 19-28 years whilst $^{14}C$ results identify three possible recharge zones at Z19486, Z20129 and Z19485.

The spatial distribution of chloride in the MSA shows that recharge occurs across the aquifer at varying rates controlled by lithology and hydraulic conductivity. Areas of low chloride content

are linked to high recharge rate while areas of high chloride content are linked to low recharge rates. This concept is further supported by the calculated recharge values from the CMB method, which shows lowest recharge rate of 4 mm/annum at Z19486 ( $Cl^-$ = 127 mg/l; K = 0.38 m/day) and highest recharge rate of 10 mm/annum at Z19485 ( $Cl^-$ = 54 mg/l; K = 1.55 m/day).

The type of overlying strata and tectonic structures in this area play a profound role in the both groundwater age and recharge conditions. In highland area where the basalts are thick and heavily fractured, these structures act as conduits leading to dissolution of basaltic rock. This fact is supported by tritium age of 39.4 years which is observed on two boreholes (Z19493 and Z20146) situated on opposite sides of the Makhujwane faults. The same age is also observed in areas where the sandstone is unconfined and at the contact between the basalt and the sandstone. In low lands were groundwater flow and hydraulic conductivities are low, < 1 m/day, infiltration occurs but precipitation quantity is not significant enough to cause a profound effect in the groundwater composition. A reasonable hypothesis is that the water gets collected in perched aquifers.

## 5.2 Recommendations

Information on the bulk rock composition could in future assist in the interpretation of the deriving geochemical reactions in this aquifer. Therefore it is recommended that thin sections and X-ray diffraction analyses of the host rock be considered in future. Some of the hypothesis presented in the paper can be cleared by conducting drilling activities that involves measurement of water chemistry at different depths and formations and placing a few boreholes in areas that are not heavily affected by faults to minimise mixing effects. Water sampling for isotope analysis should be included in the groundwater quality monitoring sampling routine.

References

Anderson, T.W. (1984). An introduction to multivariate statistical analysis. Wiley, New York, 675pp

Appelo, C and Postma , D. (1993). Geochemistry, groundwater and pollution. Balkema, Rotterdam, 536pp

Bakari, S. S., Aagaard, P., Vogt, R. D., Ruden, F., Johansen, I., Vuai, S. A. (2012). Delineation of groundwater provenance in a coastal aquifer using statistical and isotopic methods, Southeast Tanzania. *Environmental Earth Sciences*, *66*(3), 889-902.

Bamisaiye, O. A. (2015). Geo-spatial mapping of the western Bushveld Rusternburg layered suite (Rls) in South Africa. Journal of geography and geology 7(4), 88.

Beekman, H.E., Selaolo. E.T., Van Elswijk, R.C., Lenderink,N., Obakeng, O.T.O.(1997). Chloride and isotope tracing profiling in the Letlhakeng-Botlhapatlou area and the central Kalahari. GRESII technical report, 112pp

Belkhiri, L., Boudoukha, A., Mouni, L. (2011). A multivariate statistical analysis of groundwater chemistry data. International Journal of Environmental Research, 5(2), 537-544.

Boronina, A., Balderer, W., Renard, P., Stichler, W. (2005). Study of stable isotopes in the Kouris catchment (Cyprus) for the description of the regional groundwater flow. Journal of Hydrology, 308(1-4), pp.214-226.

Carney, J.N., Aldiss, D.T. and Lock, N.P. (1994). The geology of Botswana. Bulletin of the Geological Survey of Botswana, 37, 113pp.

Craig, H. (1961). Isotopic variation in meteoric waters. Science, 133: 170-1703

Clark, I. D and Fritz, P. (1997). Environmental isotopes in hydrogeology. Lewis , New York,328pp

Dansgaard, W. (1964). Stable isotopes in precipitation. Tellus, *16*(4), 436-468.

Dalton, M. G. and Upchurch, S. B. (1978). Interpretation of hydrochemical facies by factor analysis. Ground water, 16(4), 228-233.

Davis, J. (2002).Statistics and data analysis in geology, Wiley, New York

Department of Geological Surveys. (1988). Mmamabula groundwater resource investigation-Phase I, Final report, Republic of Botswana, 143pp.

Department of Geological Surveys (1994). Mmamabula groundwater resource investigation Phase II-Khurutse area, Final report, Republic of Botswana, 102pp.

Department of Geological Surveys (1984). The Lithography of the Karoo Supergroup in Botswana, Bulletin 26, by R.A. Smith

Department of Water Affairs (1984). Eastern Botswana regional Water supply Study

Department of Water Affairs (2006). National water master plan review final report. Volume 10

De Vries, J.J., Selaolo, E.T., Beekman, H.E. (2000). Groundwater recharge in the Kalahari, with reference to paleo-hydrologic conditions. Journal of Hydrology, 238(1), pp.110-123Dincer, T., Hutton, L. G., Kupee, B. B. J. (1979). Study using stable isotopes, of flow distribution, surface/groundwater relations and evapotranspiration in the Okarango Swamp, Botswana. Isotope Hydrology 1978, IAEA, Vienna, 1, 3-26.

Domenico, P. A. and Schwartz, F. W. (1990). Physical and chemical hydrogeology. Physical and chemical hydrogeology.Wiley.New York, 824pp

Duplessis, C.P and Walraven, F. (1990). The tectonic setting of the Bushveld Complex in Southern Africa ; Part I, Structural deformation and technophysics 179.

Edmunds, W.M., Darling, W.G. and Kinniburgh, D.G. (1988). Solute profile techniques for recharge estimation in semi-arid and arid terrain (pp. 139-157). Springer Netherlands.

Eichinger, L. (1983). A contribution to the interpretation of 14C groundwater ages considering the example of a partially confined sandstone aquifer: Radiocarbon, v. 25, p. 347–356.

Fontes, J. C and Garnier, J. M. (1979). Determination of the initial 14C activity of the total dissolved carbon: A review of the existing models and a new approach. Water resources research, 15(2), 399-413.

Freeze, R.A and Cherry J.A. (1979). Groundwater. Prentice-Hall, Englewood Cliffs

Geoworld., ( 2010). Consultancy for drilling and test pumping of 17 production boreholes, Groundwater Modelling - Final Technical Report, 103pp.

Ghesquière, O., Walter, J., Chesnaux, R., and Rouleau, A. (2015). Scenarios of groundwater chemical evolution in a region of the Canadian Shield based on multivariate statistical analysis. *Journal of Hydrology*, *4*, 246-266.

Han, L.-F., Plummer, L.N., Aggarwal, P. (2012). A graphical method to evaluate predominant geochemical processes occurring in groundwater systems for radiocarbon dating: Chemical Geology 318-319, p. 88–112.

Helena, B., Pardo, R., Vega, M., Barrado, E., Fernandez, J. M., Fernandez, L. (2000). Temporal evolution of groundwater composition in an alluvial aquifer (Pisuerga River, Spain) by principal component analysis. Water research, 34(3), 807-816.

Hem, J. D. (1985). Study and interpretation of the chemical characteristics of natural water (Vol. 2254). Department of the Interior, US Geological Survey.

Hussin, N. H., Yusoff, I., Tahir, W. Z. W. M., Mohamed, I., Ibrahim, A. I. N., Rambli, A. (2016). Multivariate statistical analysis for identifying water quality and hydrogeochemical evolution of shallow groundwater in Quaternary deposits in the Lower Kelantan River Basin, Malaysian Peninsula. *Environmental Earth Sciences*, *75*(14), 1-16.

.

Jassas, H. A and Merkel, B. J. (2015). Investigating groundwater recharge by means of stable isotopes in the Al-Khazir Gomal Basin, northern Iraq.Environmental Earth Sciences, 73(12), 8533 -8546.

Jennings, C. (1970). Contribution of environmental tritium measurements to some geohydrological problems in Southern Africa. Isotope Hydrology, p.289.

Leaney, F. and Allison, G. (1986). Carbon-14 and stable isotope data for an area in the Murray Basin: Its use in estimating recharge. Journal of Hydrology, 88(1-2), pp.129 -145.

Keller, S. (1988). Assessment of the groundwater potential of the Waterberg area east of Mochudi (Southeast Botswana). Unpubl. report SK/4/88. Department of Geological Surveys.

Lawrence, F. W and Upchurch, S. B. (1982). Identification of recharge areas using geochemical factor analysis. Ground Water, 20(6), 680 -687.

Mazor, E. (1982): Rain recharge in the Kalahari - a note on some approaches to the problem. J. Hydrology 55, 137-144.

Mazor, E., Bielsky, M., Verhagen, B.Th., Sellschop, J.P.F., Hutton, L., Jones, M.T. (1980). Chemical composition of groundwaters in the vast Kalahari flat land. J. of Hydrology, 48, 147-165

Mazor, E., Verhagen, B.Th., Sellschop, J.P.F. (1974): Kalahari groundwaters - their hydrogen, carbon and oxygen isotopes. Symp. on Isotope Techniques in Groundwater Hydrology, IAEA, Vienna, 1974.

Mazor, E., Verhagen, B.Th., Sellschop, J.P.F. (1977): Northern Kalahari groundwaters; hydrological, isotopic and chemical studies at Orapa, Botswana, J. of Hydrology, 34, 203-234.

Mazor, E., Vuataz, F.D., Jaffe', F. C. (1985): Tracing groundwater components by chemical, isotopic and physical parameters - example: Schinznach, Switzerland. J. of Hydrology, 76, 233-246.

Mook, W.G. (1980) Carbon-14 in hydrogeological studies. In: Handbook of environmental isotope geochemistry (Fritz, P, and Fontes, J.C., editors), Vol 1, Elsevier Sci. Publ. Co., Amsterdam, 49-74.

Mook, W.G. (1976), The dissolution-exchange model for dating groundwater with 14C, In Interpretation of Environmental Isotope and Hydrochemical Data in Groundwater Hydrology: International Atomic Energy Agency, Vienna, p. 213–225.

Moya, C. E., Raiber, M., Taulis, M., Cox, M. E. (2015). Hydrochemical evolution and groundwater flow processes in the Galilee and Eromanga basins, Great Artesian Basin, Australia: a multivariate statistical approach. *Science of The Total Environment*, *508*, 411-426.

Papatheodorou, G., Lambrakis, N., Panagopoulos, G. (2007). Application of multivariate statistical procedures to the hydrochemical study of coastal aquifers: an example from Crete, Greece. Hydrol Processes 21:1482-1495

Phillips, F.M. (1981). Noble gases in groundwater as paleo-climatic indicators, PHD Dissertation, Department of hydrology and Water Resources, University of Arizona, Tucson, 189pp

Plummer, L.N., and Glynn, P.D. (2013), Radiocarbon Dating in Groundwater Systems, In IAEA, 2013, Isotope Methods for Dating Old Groundwater, International Atomic Energy Agency, Vienna, April, 2013: Chap. 4, p. 33–89. STI/PUB/1587, ISBN 978–92–0–137210–9, 357p. http://www-pub.iaea.org/books/IAEABooks/8880/Isotope-Methods-for-Dating-Old-Groundwater.

Sami, K. (1992). Recharge mechanisms and geochemical processes in a semi-arid sedimentary basin, Eastern Cape, South Africa. Journal of Hydrology, 139(1-4), 27-48.

Selaolo, E.T.(1998). Tracer studies and groundwater recharge assessment in the eastern fringe of the Botswana Kalahari: the Letlhakeng-Botlhapatlou area. ET Selaolo.

Smith, R.A. (1984). The lithostratigraphy of the Karoo super group in Botswana (*Bulletin 26*). Department of Geological Surveys. Botswana .239pp

Stephenson, D., Shemang, E. M., Chaoka, T. R. (Eds.). (2004). Water resources of arid areas. AA Balkema Publishers.573pp

Subyani, A. M., and Al Ahmadi, M. E. (2010). Multivariate statistical analysis of groundwater quality in Wadi Ranyah, Saudi Arabia. Earth Sciences, 21(2).

Tamers, M. A. (1975). Validity of radiocarbon dates on groundwater: Geophysical Surveys, v. 2, p. 217–239.

Tessema, A., Mengistu, H., Chirenje, E., Abiye, T.A., Demlie, M. B. (2012). The relationship between lineaments and borehole yield in North West Province, South Africa: results from geophysical studies. Hydrogeology Journal, 20(2), 351 -368.

Vandenschrick, G., van Wesemael, B., Frot, E., Pulido-Bosch, A., Molina, L., Stiévenard, M., Souchez, R. (2002). Using stable isotope analysis (δD–δ18O) to characterise the regional hydrology of the Sierra de Gador, south east Spain. Journal of Hydrology, 265(1 -4), pp. 43 - 55.

Verhagen, B.T. (1990). Isotope hydrology of the Kalahari: recharge or no recharge. Paleoecology of Africa, 21, pp. 143 -158.

Verhagen, B.Th., Mazor, E., Sellschop, J.P.F. (1974): Radiocarbon and tritium evidence for direct recharge to groundwaters in the Northern Kalahari. Nature, 249, 643-644

Verhagen, B.Th., Mazor, E., Sellschop, J.P.F., Jones, M.T., Robins, N.S., Hutton, L., Jennings, C.M.H. (1975). Groundwaters of Orapa (Northern Kalahari) - Hydrological, chemical and tritium data. NPRU publication no. 75/12, University of the Witwatersrand.

Vogel, J.C., Talma, A.S., Heaton T.H.E. (1982). The age and isotopic composition of groundwater in the Stampriet Artesian Basin, SWA. National Physical Research Laboratory, CSIR, Pretoria, South Africa, 49pp.

Wallick, E. I. (1973). Isotopic and chemical considerations in radiocarbon dating of groundwater within the semi-arid Tucson Basin, Arizona. PHD Dissertation, University of Arizona,184pp

Ward, R.C. and Robinson, M. (2000). Principles of hydrology. McGraw-Hill, London, 441pp

Water Surveys Botswana. (2015a). Contract for drilling and test pumping of 8 production boreholes in Masama-Makhujwane Wellfield Replacement boreholes Masrep-1 to Masrep-4 and Mak-16-Mak-19 and an additional 2 boreholes(Re-Drill Bh8321& Z10452) ,Final Report,279pp

Water Surveys Botswana (2015b). Drilling and test pumping of 8 production boreholes at Masama-Makhujwane Wellfields, Groundwater resource quantification using Numerical Modelling, Final Report, 60pp

Winter, T. C., Mallory, S. E., Allen, T. R. and Rosenberry, D. O. (2000). The use of principal component analysis for interpreting ground water hydrographs. Ground Water, 38(2), 234.

Yeh, H. F., Lee, C. H., Hsu, K. C., Chang, P. H., Wang, C. H. (2009). Using stable isotopes for assessing the hydrologic characteristics and sources of groundwater recharge. J Environ Eng Manage, 19(4), 185 -191.

# APPENDIX A: BOREHOLE CONSTRUCTION DETAILS AND LITHOLOGY DESCRIPTION

| Borehole ID | Coordinates | | elevation | Completion Date | Depth | casing | | | | Water Strike | RWL | Lithology | | | Confined/ unconfined |
|---|---|---|---|---|---|---|---|---|---|---|---|---|---|---|---|
| | X | Y | (m) | | (mbgl) | diameter | type | depth (m) From | to | depth (m) | (mbgl) | from | to | Log | |
| Z19485 | 7360347 | 445446 | 926 | 16/05/2014 | 184 | 22" | plain steel | 0.0 | 5 | 55 | 50 | 0 | 6 | Kalahari | confined |
| | | | | | | 15" | plain steel | 0.0 | 48 | 94 | | 6 | 49 | Basalt | |
| | | | | | | 10" | plain steel | -1.0 | 97.7 | 121 | | 49 | 174 | Sandstone | |
| | | | | | | 10" | louvered screen | 97.7 | 119.7 | 139 | | 174 | 184 | Siltstone /Mudstone | |
| | | | | | | 10" | plain steel | 119.7 | 125.8 | 148 | | | | | |
| | | | | | | 10" | louvered screen | 125.8 | 169.8 | 158 | | | | | |
| | | | | | | 10" | plain steel | 169.8 | 182.0 | 175 | | | | | |
| | | | | | | 10" | open hole | 182.0 | 184.0 | | | | | | |
| Z19486 | 7350977 | 484520 | 917 | 04/06/2014 | 149 | 22" | plain steel | 0.0 | 4.1 | 66 | 33.3 | 0 | 8 | Kalahari | Unconfined |
| | | | | | | 15" | plain steel | 0.0 | 29.1 | 77 | | 8 | 141 | Sandstone | |
| | | | | | | 10" | plain steel | 1.0 | 66.8 | 140 | | 141 | 149 | Siltstone /mudstone | |
| | | | | | | 10" | louvered screen | 66.8 | 83.3 | 149 | | | | | |
| | | | | | | 10" | plain steel | 83.3 | 89.6 | | | | | | |

| Borehole ID | Coordinates | | elevation | Completion Date | Depth | casing | | | | Water Strike | RWL | Lithology | | | Confined/ unconfined |
|---|---|---|---|---|---|---|---|---|---|---|---|---|---|---|---|
| | X | Y | (m) | | (mbgl) | diameter | type | depth (m) From | to | depth (m) | (mbgl) | from | to | Log | |
| | | | | | | 10" | louvered screen | 89.6 | 138.9 | | | | | | |
| | | | | | | 10" | plain steel | 138.9 | 145.0 | | | | | | |
| | | | | | | 15" | open hole | 145.0 | 149.0 | | | | | | |
| Z19487 | 7354828 | 486718 | 917 | 06/06/2014 | 234 | 24" | plain steel | 0.0 | 4.7 | 104 | 47 | 0 | 8 | Kalahari | Confined |
| | | | | | | 22" | plain steel | -0.2 | 15.0 | 113 | | 8 | 32 | Weathered basalt | |
| | | | | | | 15" | plain steel | -0.6 | 38.0 | 220 | | 32 | 112 | Fresh basalt | |
| | | | | | | 10" | plain steel | -1.0 | 104.0 | | | 112 | 228 | Sandstone | |
| | | | | | | 10" | louvered screen | 104.0 | 137.0 | | | 228 | 234 | Siltstone /Mudstone | |
| | | | | | | 10" | plain steel | 137.0 | 161.4 | | | | | | |
| | | | | | | 10" | louvered screen | 161.4 | 166.9 | | | | | | |
| | | | | | | 10" | plain steel | 166.9 | 173.0 | | | | | | |
| | | | | | | 10" | louvered screen | 173.0 | 184.0 | | | | | | |
| | | | | | | 10" | plain steel | 184.0 | 196.2 | | | | | | |
| | | | | | | 10" | louvered screen | 196.2 | 201.7 | | | | | | |
| | | | | | | 10" | plain steel | 201.7 | 207.8 | | | | | | |

# INTEGRATED INVESTIGATION OF MASAMA SANDSTONE AQUIFER

| Borehole ID | Coordinates | | elevation | Completion Date | Depth | casing | | | | Water Strike | RWL | Lithology | | | Confined/ unconfined |
|---|---|---|---|---|---|---|---|---|---|---|---|---|---|---|---|
| | X | Y | (m) | | (mbgl) | diameter | type | depth (m) From | depth (m) to | depth (m) | (mbgl) | from | to | Log | |
| | | | | | | 10" | louvered screen | 207.8 | 224.3 | | | | | | |
| | | | | | | 10" | plain steel | 224.3 | 230.4 | | | | | | |
| | | | | | | 15" | open hole | 230.4 | 234.0 | | | | | | |
| Z19489 | 7346635 | 439163 | 908 | 25/06/2014 | 436 | 24" | plain steel | 0.0 | 6.0 | 299 | 44 | 0 | 26 | Kalahari | Confined |
| | | | | | | 22" | plain steel | 0.0 | 26.0 | 319 | | 26 | 41 | Weathered basalt | |
| | | | | | | 15" | plain steel | 0.0 | 41.0 | 337 | | 41 | 292 | Fresh basalt | |
| | | | | | | 10" | plain steel | -0.9 | 291.9 | | | 292 | 427 | Sandstone | |
| | | | | | | 10" | louvered screen | 291.9 | 313.9 | | | 427 | 436 | Siltstone /Mudstone | |
| | | | | | | 10" | plain steel | 313.9 | 326.1 | | | | | | |
| | | | | | | 10" | louvered screen | 326.1 | 342.6 | | | | | | |
| | | | | | | 10" | plain steel | 342.6 | 354.8 | | | | | | |
| | | | | | | 10" | louvered screen | 354.8 | 409.8 | | | | | | |
| | | | | | | 10" | plain steel | 409.8 | 415.9 | | | | | | |
| | | | | | | 10" | louvered screen | 415.9 | 426.9 | | | | | | |
| | | | | | | 10" | plain steel | 426.9 | 433.0 | | | | | | |

| Borehole ID | Coordinates | | elevation | Completion Date | Depth | casing | | | | Water Strike | RWL | Lithology | | | Confined/ unconfined |
|---|---|---|---|---|---|---|---|---|---|---|---|---|---|---|---|
| | X | Y | (m) | | (mbgl) | diameter | type | depth (m) From | to | depth (m) | (mbgl) | from | to | Log | |
| | | | | | | 15" | open hole | 433.0 | 436.0 | | | | | | |
| Z19490 | 7360468 | 441220 | | 27/06/2014 | 161 | 24" | plain steel | 0.0 | 3.4 | 75 | 58 | 0 | 5 | Kalahari | Unconfined |
| | | | | | | 22" | plain steel | 0.0 | 18.4 | 87 | | 5 | 22 | Weathered basalt | |
| | | | | | | 15" | plain steel | 0.0 | 35.9 | 106 | | 22 | 150 | Sandstone | |
| | | | | | | 10" | plain steel | -1.0 | 100.0 | 120 | | 150 | 161 | Siltstone /Mudstone | |
| | | | | | | 10" | louvered screen | 100.0 | 155.0 | 135 | | | | | |
| | | | | | | 10" | plain steel | 155.0 | 158.0 | 144 | | | | | |
| | | | | | | 15" | open hole | 158.0 | 161.0 | | | | | | |
| Z19493 | 7348104 | 437318 | | 23/08/2014 | 471 | 24" | plain steel | 0.0 | 4.8 | 363 | 51.58 | 0 | 29 | Kalahari | Confined |
| | | | | | | 22" | plain steel | -0.5 | 29.4 | 371 | | 29 | 54 | Weathered basalt | |
| | | | | | | 15" | plain steel | -0.4 | 59.0 | | | 54 | 363 | Fresh basalt | |
| | | | | | | 10" | plain steel | -1.0 | 365.9 | | | 363 | 471 | Ntane sandstone | |
| | | | | | | 10" | louvered screen | 365.9 | 464.0 | | | | | | |
| | | | | | | 10" | plain steel | 464.0 | 467.0 | | | | | | |

| Borehole ID | Coordinates | | elevation | Completion Date | Depth | casing | | | | Water Strike | RWL | Lithology | | | Confined/ unconfined |
|---|---|---|---|---|---|---|---|---|---|---|---|---|---|---|---|
| | X | Y | (m) | | (mbgl) | diameter | type | depth (m) From | to | depth (m) | (mbgl) | from | to | Log | |
| | | | | | | 15" | open hole | 467.0 | 471.0 | | | | | | |
| Z20129 | 7355131 | 440343 | 951 | 2-6/12/2014 | 176 | 24" | plain steel | 0.0 | 5.0 | 59 | 54.6 | 0 | 18 | Kalahari | Unconfined |
| | | | | | | 15" | plain steel | 0.0 | 41.0 | 113 | | 18 | 133 | Sandstone | |
| | | | | | | 10" | plain steel | -1.0 | 105.0 | 176 | | 133 | 176 | Mudstone | |
| | | | | | | 10" | louvered screen | 105.0 | 149.0 | | | | | | |
| | | | | | | 10" | plain steel | 149.0 | 155.1 | | | | | | |
| | | | | | | 15" | open hole | 155.1 | 176.0 | | | | | | |
| Z20131 | 7359414 | 441462 | 952 | 02/11/2014 | 214 | 24" | plain steel | 0.0 | 5.5 | 84 | 63.31 | 0 | 14 | Kalahari | Confined |
| | | | | | | 22" | plain steel | -0.3 | 36.0 | 94 | | 14 | 63 | Basalt | |
| | | | | | | 15" | plain steel | -0.5 | 58.0 | 103 | | 49 | 211 | Sandstone | |
| | | | | | | 10" | plain steel | -1.0 | 103.0 | 139 | | 211 | 124 | Mudstone | |
| | | | | | | 10" | louvered screen | 103.0 | 147.0 | 157 | | | | | |
| | | | | | | 10" | plain steel | 147.0 | 153.1 | | | | | | |
| | | | | | | 10" | louvered screen | 153.1 | 202.6 | | | | | | |

| Borehole ID | Coordinates | | elevation | Completion Date | Depth | casing | | | | Water Strike | RWL | Lithology | | | Confined/ unconfined |
|---|---|---|---|---|---|---|---|---|---|---|---|---|---|---|---|
| | X | Y | (m) | | (mbgl) | diameter | type | depth (m) From | to | depth (m) | (mbgl) | from | to | Log | |
| | | | | | | 10" | plain steel | 202.6 | 208.7 | | | | | | |
| | | | | | | 15" | open hole | 208.7 | 214.0 | | | | | | |
| Z20133 | 7361040 | 441489 | 956 | 13/12/2014 | 210 | 24" | plain steel | 0.0 | 2.0 | 129 | 62.27 | 0 | 8 | Kalahari | Confined |
| | | | | | | 22" | plain steel | 0.0 | 12.0 | 201 | | 8 | 30 | Basalt | |
| | | | | | | 15" | plain steel | 0.0 | 32.0 | | | 30 | 199 | Sandstone | |
| | | | | | | 10" | plain steel | -1.0 | 103.0 | | | 199 | 210 | Mudstone | |
| | | | | | | 10" | louvered screen | 103.0 | 147.0 | | | | | | |
| | | | | | | 10" | plain steel | 147.0 | 153.1 | | | | | | |
| | | | | | | 10" | louvered screen | 153.1 | 202.6 | | | | | | |
| | | | | | | 10" | plain steel | 202.6 | 208.7 | | | | | | |
| | | | | | | 15" | open hole | 208.7 | 210.0 | | | | | | |
| | | | | | | | | | | | | | | | |
| Z20137 | 7356983 | 444119 | 944 | 26/01/2015 | 237 | 24" | plain steel | 0.0 | 5.0 | 75 | 49.88 | 0 | 5 | Kalahari | Confined |
| | | | | | | 22" | plain steel | 0.0 | 12.0 | 93 | | 5 | 13 | Basalt | |
| | | | | | | 15" | plain steel | 0.0 | 48.0 | 147 | | 13 | 232 | Sandstone | |

| Borehole ID | Coordinates | | elevation | Completion Date | Depth | casing | | | | Water Strike | RWL | Lithology | | | Confined/ unconfined |
|---|---|---|---|---|---|---|---|---|---|---|---|---|---|---|---|
| | X | Y | (m) | | (mbgl) | diameter | type | depth (m) From | to | depth (m) | (mbgl) | from | to | Log | |
| | | | | | | 10" | plain steel | -1.0 | 74.0 | 201 | | 232 | 237 | Siltstone/Mudstone | |
| | | | | | | 10" | louvered screen | 74.0 | 107.0 | 219 | | | | | |
| | | | | | | 10" | plain steel | 107.0 | 119.2 | | | | | | |
| | | | | | | 10" | louvered screen | 119.2 | 152.2 | | | | | | |
| | | | | | | 10" | plain steel | 152.2 | 164.4 | | | | | | |
| | | | | | | 10" | louvered screen | 164.4 | 202.9 | | | | | | |
| | | | | | | 10" | plain steel | 202.9 | 233.4 | | | | | | |
| | | | | | | 15" | open hole | 233.4 | 237.0 | | | | | | |
| Z20138 | 7356387 | 446996 | 926 | 21/02/2015 | 180 | 24" | plain steel | 0.0 | 5.0 | 76 | 51.65 | 0 | 9 | Kalahari | Unconfined |
| | | | | | | 22" | plain steel | 0.0 | 10.7 | 88 | | 9 | 156 | Sandstone | |
| | | | | | | 15" | plain steel | 0.0 | 42.0 | 112 | | 156 | 180 | Siltstone/Mudstone | |
| | | | | | | 10" | plain steel | -1.0 | 70.0 | | | | | | |
| | | | | | | 10" | louvered screen | 70.0 | 120.0 | | | | | | |
| | | | | | | 10" | plain steel | 120.0 | 126.0 | | | | | | |
| | | | | | | 10" | louvered screen | 126.0 | 165.0 | | | | | | |

| Borehole ID | Coordinates | | elevation | Completion Date | Depth | casing | | | | Water Strike | RWL | Lithology | | | Confined/ unconfined |
|---|---|---|---|---|---|---|---|---|---|---|---|---|---|---|---|
| | X | Y | (m) | | (mbgl) | diameter | type | depth (m) From | to | depth (m) | (mbgl) | from | to | Log | |
| | | | | | | 10" | plain steel | 165.0 | 177.2 | | | | | | |
| | | | | | | 15" | open hole | 177.2 | 180.0 | | | | | | |
| Z20141 | 7365610 | 451410 | 938 | 14/02/2015 | 181 | 24" | plain steel | 0.0 | 7.1 | 71 | 44.35 | 0 | 5 | Kalahari | Unconfined |
| | | | | | | 22" | plain steel | 0.0 | 12.2 | 90 | | 5 | 9 | Basalt | |
| | | | | | | 15" | plain steel | 0.0 | 42.6 | 140 | | 9 | 181 | Sandstone | |
| | | | | | | 10" | plain steel | -1.0 | 67.5 | 170 | | | | | |
| | | | | | | 10" | louvered screen | 67.5 | 117.0 | 181 | | | | | |
| | | | | | | 10" | plain steel | 117.0 | 123.1 | | | | | | |
| | | | | | | 10" | louvered screen | 123.1 | 167.1 | | | | | | |
| | | | | | | 10" | plain steel | 167.1 | 173.2 | | | | | | |
| | | | | | | 15" | open hole | 173.2 | 181.0 | | | | | | |
| Z20143 | 7360828 | 451729 | 927 | 20/02/2015 | 201 | 24" | plain steel | 0.0 | 5.0 | 111 | 49 | 0 | 7 | Kalahari | Unconfined |
| | | | | | | 22" | plain steel | 0.0 | 11.5 | 120 | | 7 | 16 | Basalt | |
| | | | | | | 15" | plain steel | 0.0 | 45.0 | 134 | | 16 | 196 | Sandstone | |

| Borehole ID | Coordinates | | elevation | Completion Date | Depth | casing | | | | Water Strike | RWL | Lithology | | | Confined/ unconfined |
|---|---|---|---|---|---|---|---|---|---|---|---|---|---|---|---|
| | X | Y | (m) | | (mbgl) | diameter | type | depth (m) From | to | depth (m) | (mbgl) | from | to | Log | |
| | | | | | | 10" | plain steel | 0.0 | 118.0 | 147 | | 196 | 201 | Mudstone | |
| | | | | | | 10" | louvered screen | 118.0 | 189.5 | 183 | | | | | |
| | | | | | | 10" | plain steel | 189.5 | 195.6 | 201 | | | | | |
| | | | | | | 15" | open hole | 195.6 | 201.0 | | | | | | |
| Z20145 | 7358053 | 453626 | 935 | 11/03/2015 | 155 | 24" | plain steel | 0.0 | 4.8 | 57 | 44.83 | 0 | 3 | Kalahari | Confined |
| | | | | | | 22" | plain steel | 0.0 | 30.0 | 86 | | 3 | 50 | Basalt | |
| | | | | | | 15" | plain steel | 0.0 | 48.8 | 108 | | 50 | 142 | Sandstone | |
| | | | | | | 10" | plain steel | -1.0 | 62.0 | 116 | | 142 | 155 | Mudstone | |
| | | | | | | 10" | louvered screen | 62.0 | 117.0 | 155 | | | | | |
| | | | | | | 10" | plain steel | 117.0 | 123.1 | | | | | | |
| | | | | | | 10" | louvered screen | 123.1 | 145.1 | | | | | | |
| | | | | | | 10" | plain steel | 145.1 | 151.2 | | | | | | |
| | | | | | | 15" | open hole | 151.2 | 155.0 | | | | | | |
| Z20146 | 437458 | 734964 | 920 | 28/02/2015 | 252 | 24" | plain steel | 0.0 | 1.7 | 156 | 42 | 0 | 21 | Kalahari | Confined |
| | | | | | | 22" | plain steel | 0.0 | 23.7 | 185 | | 21 | 119 | Basalt | |

| Borehole ID | Coordinates | | elevation | Completion Date | Depth | casing | | | | Water Strike | RWL | Lithology | | | Confined/ unconfined |
|---|---|---|---|---|---|---|---|---|---|---|---|---|---|---|---|
| | X | Y | (m) | | (mbgl) | diameter | type | depth (m) From | to | depth (m) | (mbgl) | from | to | Log | |
| | | | | | | 15" | plain steel | 0.0 | 48.8 | 226 | | 119 | 237 | Sandstone | |
| | | | | | | 10" | plain steel | -1.0 | 152.5 | | | 237 | 252 | Mudstone | |
| | | | | | | 10" | louvered screen | 152.5 | 240.5 | | | | | | |
| | | | | | | 10" | plain steel | 240.5 | 246.6 | | | | | | |
| | | | | | | 15" | open hole | 246.6 | 252.0 | | | | | | |
| Z20147 | 435463 | 7349386 | 934 | 14/03/2015 | 339 | 24" | plain steel | 0.0 | 3.9 | 205 | 46.2 | 0 | 30 | Kalahari | Confined |
| | | | | | | 22" | plain steel | 0.0 | 29.2 | 225 | | 30 | 205 | Basalt | |
| | | | | | | 15" | plain steel | 0.0 | 75.5 | 255 | | 205 | 339 | Sandstone | |
| | | | | | | 10" | plain steel | -1.0 | 212.0 | 267 | | | | | |
| | | | | | | 10" | louvered screen | 212.0 | 267.0 | 303 | | | | | |
| | | | | | | 10" | plain steel | 267.0 | 273.1 | | | | | | |
| | | | | | | 10" | louvered screen | 273.1 | 328.1 | | | | | | |
| | | | | | | 10" | plain steel | 328.1 | 334.2 | | | | | | |
| | | | | | | 10" | open hole | 334.2 | 339.0 | | | | | | |

| Borehole ID | Coordinates | | elevation | Completion Date | Depth | casing | | | | Water Strike | RWL | Lithology | | | Confined/ unconfined |
|---|---|---|---|---|---|---|---|---|---|---|---|---|---|---|---|
| | X | Y | (m) | | (mbgl) | diameter | type | depth (m) From | to | depth (m) | (mbgl) | from | to | Log | |
| BH11160 | 7362107 | 430467 | 951 | 19/04/2016 | 247 | 24" | plain steel | 0.0 | 12.9 | | 60.6 | 0 | 25 | Kalahari | Confined |
| | | | | | | 22" | plain steel | 0.0 | 26.1 | | | 25 | 117 | Basalt | |
| | | | | | | 15" | plain steel | 0.0 | 76.7 | | | 117 | 240 | Sandstone | |
| | | | | | | 10" | plain steel | 1.0 | 102.0 | | | 240 | 247 | Mudstone | |
| | | | | | | 10" | louvered screen | 102.0 | 113.0 | | | | | | |
| | | | | | | 10" | plain steel | 113.0 | 119.1 | | | | | | |
| | | | | | | 10" | louvered screen | 119.1 | 141.1 | | | | | | |
| | | | | | | 10" | plain steel | 141.1 | 153.3 | | | | | | |
| | | | | | | 10" | louvered screen | 153.3 | 175.3 | | | | | | |
| | | | | | | 10" | plain steel | 175.3 | 181.4 | | | | | | |
| | | | | | | 10" | louvered screen | 181.4 | 203.4 | | | | | | |
| | | | | | | 10" | plain steel | 203.4 | 215.6 | | | | | | |
| | | | | | | 10" | louvered screen | 215.6 | 237.6 | | | | | | |
| | | | | | | 10" | Plain steel | 237.6 | 243.7 | | | | | | |
| | | | | | | 15" | open hole | 243.7 | 247.0 | | | | | | |

| Borehole ID | Coordinates | | elevation | Completion Date | Depth | casing | | | | Water Strike | RWL | Lithology | | | Confined/ unconfined |
|---|---|---|---|---|---|---|---|---|---|---|---|---|---|---|---|
| | X | Y | (m) | | (mbgl) | diameter | type | depth (m) From | to | depth (m) | (mbgl) | from | to | Log | |
| BH11166 | 7357674 | 433319 | 944 | 02/06/2016 | 347 | 24" | plain steel | 0.0 | 2.4 | | 53.4 | 0 | 24 | Kalahari | Confined |
| | | | | | | 22" | plain steel | 0.0 | 26.9 | | | 24 | 200 | Basalt | |
| | | | | | | 15" | plain steel | 0.0 | 61.0 | | | 200 | 320 | Sandstone | |
| | | | | | | 10" | plain steel | +1 | 226.1 | | | 320 | 347 | Mudstone | |
| | | | | | | 10" | louvered screen | 226.1 | 237.1 | | | | | | |
| | | | | | | 10" | plain steel | 237.1 | 243.2 | | | | | | |
| | | | | | | 10" | louvered screen | 243.2 | 254.2 | | | | | | |
| | | | | | | 10" | plain steel | 254.2 | 260.3 | | | | | | |
| | | | | | | 10" | louvered screen | 260.3 | 298.8 | | | | | | |
| | | | | | | 10" | plain steel | 298.8 | 304.9 | | | | | | |
| | | | | | | 10" | louvered screen | 304.9 | 337.9 | | | | | | |
| | | | | | | 10" | plain steel | 337.9 | 344.0 | | | | | | |
| | | | | | | 15" | open hole | 344.0 | 347.0 | | | | | | |
| BH11168 | 7363146 | 427392 | 937 | 28/06/2016 | 286 | 24" | Plain steel | -0.1 | 2.0 | | 59 | 0 | 14 | Kalahari | Confined |
| | | | | | | 22" | Plain steel | -0.6 | 23.0 | | | 14 | 140 | Basalt | |

| Borehole ID | Coordinates | | elevation | Completion Date | Depth | casing | | | | Water Strike | RWL | Lithology | | | Confined/ unconfined |
|---|---|---|---|---|---|---|---|---|---|---|---|---|---|---|---|
| | X | Y | (m) | | (mbgl) | diameter | type | depth (m) From | to | depth (m) | (mbgl) | from | to | Log | |
| | | | | | | 15" | Plain steel | -0.5 | 77.0 | | | 140 | 286 | Sandstone | |
| | | | | | | 10" | Plain steel | -1.0 | 148.7 | | | | | | |
| | | | | | | 10" | louvered screen | 148.7 | 176.2 | | | | | | |
| | | | | | | 10" | Plain steel | 176.2 | 182.3 | | | | | | |
| | | | | | | 10" | louvered screen | 182.3 | 193.3 | | | | | | |
| | | | | | | 10" | Plain steel | 193.3 | 199.4 | | | | | | |
| | | | | | | 10" | louvered screen | 199.4 | 210.3 | | | | | | |
| | | | | | | 10" | Plain steel | 210.3 | 216.4 | | | | | | |
| | | | | | | 10" | louvered screen | 216.4 | 243.9 | | | | | | |
| | | | | | | 10" | Plain steel | 243.9 | 250.0 | | | | | | |
| | | | | | | 10" | louvered screen | 250.0 | 283.0 | | | | | | |
| | | | | | | 10" | Plain steel | 283.0 | 285.0 | | | | | | |
| | | | | | | 15" | open hole | 285.0 | 286.0 | | | | | | |

# APPENDIX B: SAMPLE OF BOREHOLE LOG

Borehole No : **Z19486**
Location:**Masama East**

| NORTHINGS: | EASTINGS: | *UTM Zone 35S* | TOTAL DEPTH : | GROUND SURFACE ELEVATION: |
|---|---|---|---|---|
| **7350977** | **484520** | *WGS 84* | **149m** | **917m** |
| | | | DATE STARTED: | DATE COMPLETED : |
| | | | **29/05/2014** | **04/06/2014** |

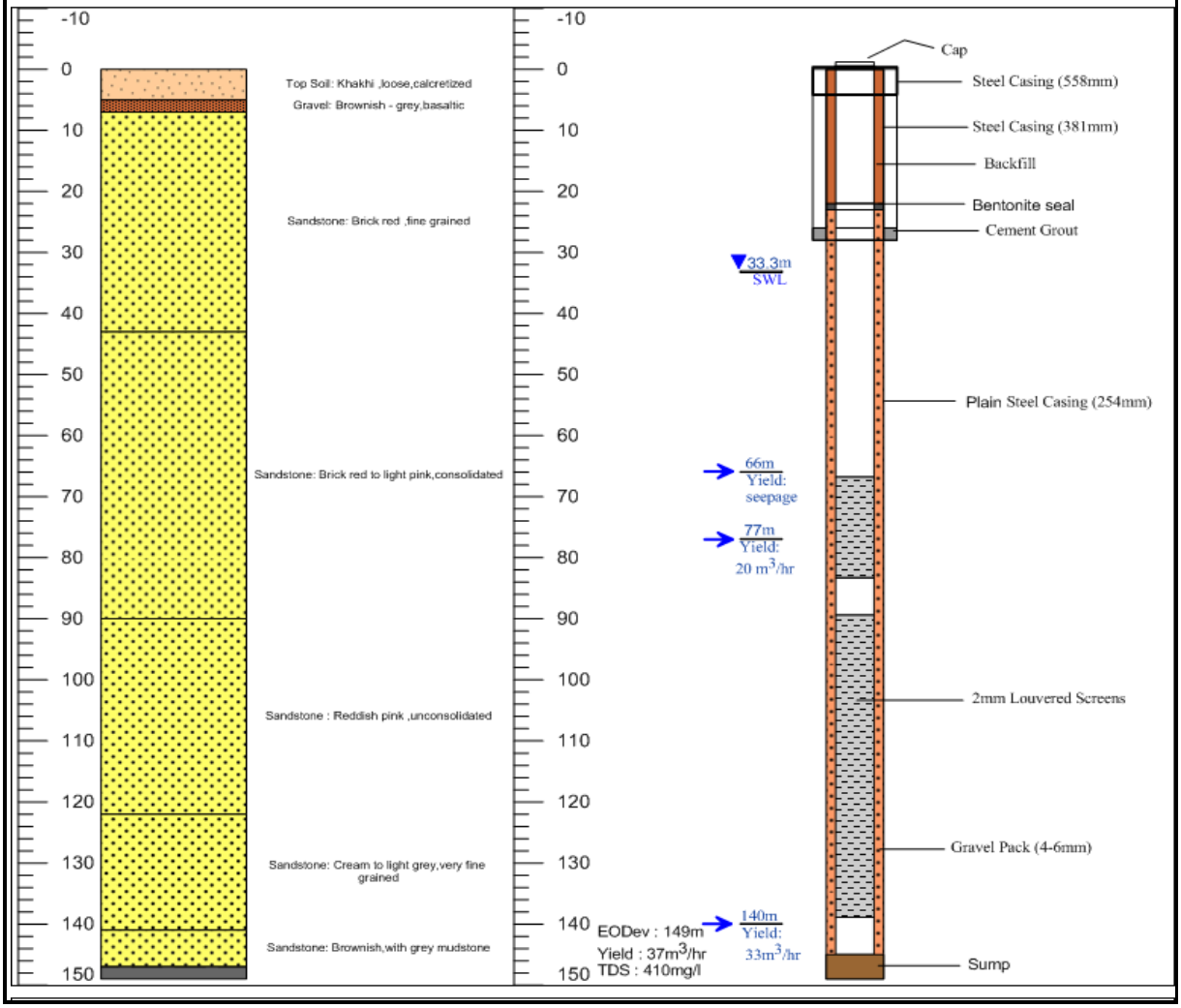

# APPENDIX C: SAMPLE OF TEST PUMPING FIELD DATA AND AQUIFER PARAMETERS CALCULATIONS

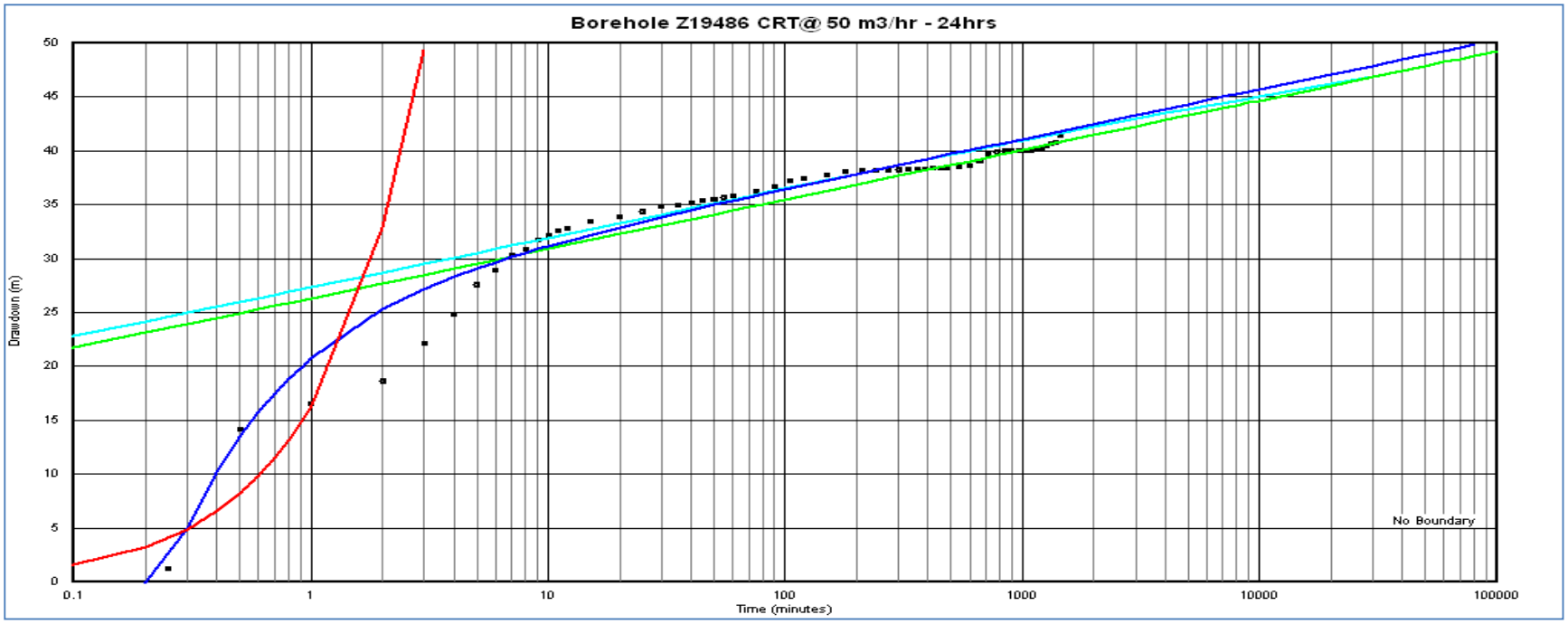


TestCurve 9.4 - [Parameters]

File Edit View Graph Window Help

<< Input | Project | Graph >>

| | | | |
|---|---|---|---|
| Pumping Rate | (>0 - 2100) | 50 | m³/hr |
| Transmissivity | (>0 - 50000) | 48 | m²/day |
| Storage coeff, early time | (>0 - 1) | 0.015 | |
| Storage coeff, late time | (>0 - 1) | 0.025 | |
| Well Diameter | (1 - 20) | 10 | inch |
| Aquifer thickness | (1 - 500) | 100 | m |
| C-value from Step Test | (0 - 1000) | 0 | h²/m5 |
| Skin Factor | (-20 - 50) | 4 | |
| Total Well-loss factor | (as skin) | 4 | |
| Aquifer interpreted | | No Boundary | |

# INTEGRATED INVESTIGATION OF MASAMA SANDSTONE AQUIFER

| | | | |
|---|---|---|---|
| **Official BH NO :** | Z19486 | District :Central | |
| Date of test commencement : | 17.6.2014 | Location :Masama | |
| Time of test commencement : | 0830hrs | BH depth(m) :149 | |
| Date of test completion | 18.6.2014 | Screen Interval (m) | |
| Time of test completion : | 0830hrs | Depth of pump intake (m) :85 | |
| Method of water level measurement | dipper | Description of MP: Top of dipper tubing | |
| OB BH NO: | 7152 | Height of MP above ground(m) :0,7 | |
| Distance ob BH r (m) | 20.7 | Static Water level before test(m) :34,19 | |
| Casing diameter (mm) | 10" | Water strike | |
| Orifice plate diameter | | Delivery pipe diameter:100mm | |
| Latitude | | Longitude | |

| clock | | Elapsed time (min) | Depth to Water (m) | Drawdown (m) | Time to fill 150l | Q($m^3$/h) | Temp ($^0$C) | EC (ms/Cm) | pH |
|---|---|---|---|---|---|---|---|---|---|
| | | 0.25 | 35.48 | 35.48 | | | | | |
| | | 0.5 | 48.37 | 48.37 | | | | | |
| | | 1 | 50.70 | 50.70 | 11.12 | 48.56 | | | |
| | | 2 | 52.84 | 52.84 | 10.39 | 51.97 | | | |
| | | 3 | 56.35 | 56.35 | 10.78 | 50.09 | | | |
| | | 4 | 58.98 | 58.98 | 10.80 | 50.00 | | | |
| | | 5 | 61.77 | 61.77 | 10.75 | 50.23 | | | |
| | | 6 | 63.07 | 63.07 | 10.79 | 50.05 | | | |

| | | | | | | | | | |
|---|---|---|---|---|---|---|---|---|---|
| | | 7 | 64.50 | 64.50 | 10.78 | 50.09 | | | |
| | | 8 | 65.08 | 65.08 | 10.80 | 50.00 | | | |
| | | 9 | 65.90 | 65.90 | 10.77 | 50.14 | | | |
| | | 10 | 66.39 | 66.39 | 10.75 | 50.23 | | | |
| | | 11 | 66.75 | 66.75 | 10.74 | 50.28 | | | |
| | | 12 | 67.03 | 67.03 | 10.80 | 50.00 | | | |
| | | 15 | 67.60 | 67.60 | 10.75 | 50.23 | 22.9 | 0.43 | 8.30 |
| | | 20 | 68.05 | 68.05 | 10.78 | 50.09 | 20.4 | 0.42 | 8.13 |
| | | 25 | 68.55 | 68.55 | 10.74 | 50.28 | 19.0 | 0.46 | 7.93 |
| | | 30 | 69.00 | 69.00 | 10.80 | 50.00 | 19.9 | 0.44 | 8.36 |
| | | 35 | 69.18 | 69.18 | 10.75 | 50.23 | 21.0 | 0.42 | 8.40 |
| | | 40 | 69.33 | 69.33 | 10.78 | 50.09 | 19.6 | 0.44 | 8.45 |
| | | 45 | 69.60 | 69.60 | 10.74 | 50.28 | 21.4 | 0.45 | 8.40 |
| | | 50 | 69.71 | 69.71 | 10.77 | 50.14 | 20.6 | 0.44 | 8.44 |
| | | 55 | 69.84 | 69.84 | 10.80 | 50.00 | 21.7 | 0.42 | 8.49 |
| | | 60 | 70.05 | 70.05 | 10.79 | 50.05 | 22.1 | 0.42 | 8.40 |
| | | 75 | 70.43 | 70.43 | 10.75 | 50.23 | 21.4 | 0.43 | 8.45 |
| | | 90 | 70.90 | 70.90 | 10.80 | 50.00 | 21.8 | 0.44 | 8.49 |
| | | 105 | 71.36 | 71.36 | 10.77 | 50.14 | 21.8 | 0.44 | 8.49 |
| | | 120 | 71.64 | 71.64 | 10.80 | 50.00 | 21.5 | 0.45 | 8.50 |
| | | 150 | 71.92 | 71.92 | 10.78 | 50.09 | 21.5 | 0.45 | 8.50 |
| | | 180 | 72.26 | 72.26 | 10.75 | 50.23 | 23.4 | 0.42 | 7.93 |
| | | 210 | 72.32 | 72.32 | 10.79 | 50.05 | 23.4 | 0.42 | 7.94 |
| | | 240 | 72.35 | 72.35 | 10.80 | 50.00 | 23.0 | 0.40 | 7.96 |
| | | 270 | 72.37 | 72.37 | 10.77 | 50.14 | 23.1 | 0.42 | 7.96 |

| | | | | | | | | | |
|---|---|---|---|---|---|---|---|---|---|
| | | 300 | 72.42 | 72.42 | 10.80 | 50.00 | 23.1 | 0.42 | 7.95 |
| | | 330 | 72.47 | 72.47 | 10.75 | 50.23 | 23.3 | 0.41 | 7.96 |
| | | 360 | 72.50 | 72.50 | 10.80 | 50.00 | 24.0 | 0.42 | 7.96 |
| | | 390 | 72.52 | 72.52 | 10.80 | 50.00 | 25.0 | 0.42 | 7.96 |
| | | 420 | 72.55 | 72.55 | 10.75 | 50.23 | 25.0 | 0.42 | 7.94 |
| | | 450 | 72.58 | 72.58 | 10.80 | 50.00 | 25.0 | 0.42 | 7.95 |
| | | 480 | 72.61 | 72.61 | 10.77 | 50.14 | 25.0 | 0.42 | 7.94 |
| | | 540 | 72.65 | 72.65 | 10.80 | 50.00 | 25 | 0.42 | 7.96 |
| | | 600 | 72.78 | 72.78 | 10.77 | 50.14 | 17.8 | 0.43 | 7.80 |
| | | 660 | 73.28 | 73.28 | 10.75 | 50.23 | 17.5 | 0.45 | 7.64 |
| | | 720 | 73.90 | 73.90 | 10.80 | 50.00 | 15.2 | 0.44 | 7.55 |
| | | 780 | 74.04 | 74.04 | 10.77 | 50.14 | 15.4 | 0.46 | 7.57 |
| | | 840 | 74.15 | 74.15 | 10.80 | 50.00 | 15.6 | 0.49 | 7.44 |
| | | 900 | 74.18 | 74.18 | 10.75 | 50.23 | 14.4 | 0.50 | 7.49 |
| | | 960 | 74.20 | 74.20 | 10.79 | 50.05 | 15.8 | 0.46 | 7.50 |
| | | 1020 | 74.22 | 74.22 | 10.80 | 50.00 | 15.6 | 0.44 | 7.54 |
| | | 1080 | 74.24 | 74.24 | 10.78 | 50.09 | 15.0 | 0.42 | 7.60 |
| | | 1140 | 74.28 | 74.28 | 10.76 | 50.19 | 10.4 | 0.43 | 7.61 |
| | | 1200 | 74.30 | 74.30 | 10.75 | 50.23 | 10.0 | 0.44 | 7.63 |
| | | 1260 | 74.66 | 74.66 | 10.80 | 50.00 | 10.1 | 0.43 | 7.65 |
| | | 1320 | 74.84 | 74.84 | 10.77 | 50.14 | 13.4 | 0.44 | 7.60 |
| | | 1380 | 74.92 | 74.92 | 10.78 | 50.09 | 17.9 | 0.30 | 7.61 |
| 1 day | | 1440 | 75.55 | 75.55 | 10.78 | 50.09 | 21.4 | 0.42 | 7.54 |

INTEGRATED INVESTIGATION OF MASAMA SANDSTONE AQUIFER

| | | | |
|---|---|---|---|
| **Official BH NO :** | Z19486 | District : | Central |
| Date of test commencement : | 17.6.2014 | Location : | Masama |
| Time of test commencement : | 0830hrs | BH depth(m) : | |
| Date of test completion | 18.6.2014 | Screen Interval (m) | |
| Time of test completion : | 0830hrs | Depth of pump intake (m) : | Observation borehole 7152 |
| Method of water level measurement | electric dipper | Description of MP | top of casing |
| OB BH NO: | 7152 | Height of MP above ground(m) : | 0.24 |
| Distance ob BH r (m) | 20.7 | Static Water level before test(m) : | 34.80 |
| Casing diameter (mm) | 10" | Water strike | |
| Orifice plate diameter | | Delivery pipe diameter | Observation borehole |
| Latitude | | Longitude | |

| clock | Elapsed time (min) | Depth to Water (m) | Drawdown (m) | Time to fill 150l | Q($m^3$/h) | Temp ($^0$C) | EC (ms/Cm) | pH | Comments |
|---|---|---|---|---|---|---|---|---|---|
| | 0.25 | 35.13 | 0.33 | | | | | | |
| | 0.5 | 35.24 | 0.44 | | | | | | |
| | 1 | 35.42 | 0.62 | | | | | | |
| | 2 | 35.71 | 0.91 | | | | | | |
| | 3 | 36.04 | 1.24 | | | | | | |
| | 4 | 36.27 | 1.47 | | | | | | |
| | 5 | 36.49 | 1.69 | | | | | | |

| | | | | | | | | | |
|---|---|---|---|---|---|---|---|---|---|
| | 6 | 36.57 | 1.77 | | | | | | |
| | 7 | 36.68 | 1.88 | | | | | | |
| | 8 | 36.77 | 1.97 | | | | | | |
| | 9 | 36.84 | 2.04 | | | | | | |
| | 10 | 36.92 | 2.12 | | | | | | |
| | 11 | 36.97 | 2.17 | | | | | | |
| | 12 | 37.01 | 2.21 | | | | | | |
| | 15 | 37.09 | 2.29 | | | | | | |
| | 20 | 37.17 | 2.37 | | | | | | |
| | 25 | 37.27 | 2.47 | | | | | | |
| | 30 | 37.27 | 2.47 | | | | | | |
| | 35 | 37.30 | 2.50 | | | | | | |
| | 40 | 37.32 | 2.52 | | | | | | |
| | 45 | 37.35 | 2.55 | | | | | | |
| | 50 | 37.36 | 2.56 | | | | | | |
| | 55 | 37.38 | 2.58 | | | | | | |
| | 60 | 37.40 | 2.60 | | | | | | |
| | 75 | 37.43 | 2.63 | | | | | | |
| | 90 | 37.45 | 2.65 | | | | | | |
| | 105 | 37.49 | 2.69 | | | | | | |
| | 120 | 37.51 | 2.71 | | | | | | |
| | 150 | 37.53 | 2.73 | | | | | | |
| | 180 | 37.55 | 2.75 | | | | | | |
| | 210 | 37.61 | 2.81 | | | | | | |
| | 240 | 37.61 | 2.81 | | | | | | |

| | | | | | | | | | |
|---|---|---|---|---|---|---|---|---|---|
| | 270 | 37.61 | 2.81 | | | | | | |
| | 300 | 37.64 | 2.84 | | | | | | |
| | 330 | 37.66 | 2.86 | | | | | | |
| | 360 | 37.68 | 2.88 | | | | | | |
| | 390 | 37.68 | 2.88 | | | | | | |
| | 420 | 37.69 | 2.89 | | | | | | |
| | 450 | 37.70 | 2.90 | | | | | | |
| | 480 | 37.71 | 2.91 | | | | | | |
| | 540 | 37.72 | 2.92 | | | | | | |
| | 600 | 37.92 | 3.12 | | | | | | |
| | 660 | 37.92 | 3.12 | | | | | | |
| | 720 | 37.92 | 3.12 | | | | | | |
| | 780 | 37.93 | 3.13 | | | | | | |
| | 840 | 37.93 | 3.13 | | | | | | |
| | 900 | 37.93 | 3.13 | | | | | | |
| | 960 | 37.94 | 3.14 | | | | | | |
| | 1020 | 37.94 | 3.14 | | | | | | |
| | 1080 | 37.95 | 3.15 | | | | | | |
| | 1140 | 37.95 | 3.15 | | | | | | |
| | 1200 | 37.96 | 3.16 | | | | | | |
| | 1260 | 37.97 | 3.17 | | | | | | |
| | 1320 | 37.97 | 3.17 | | | | | | |
| | 1380 | 37.97 | 3.17 | | | | | | |
| 1 day | 1440 | 37.97 | 3.17 | | | | | | |

WL at end of test _____(m)
Total Drawdown _____(m)
Total hours pumping _____(m)

Final discharge rate _____ (m3/h)
Quality of water _____
Water use _____

Date: _____ Signature of test pump operator: _____